Remote Sensing of Environment 332 (2026) 115027



Contents lists available at ScienceDirect

Remote Sensing of Environment

journal homepage: www.elsevier.com/locate/rse



deadtrees.earth — An open-access and interactive database for centimeter-scale aerial imagery to uncover global tree mortality dynamics

Clemens Mosig [1,2,*,a], Janusch Vajna-Jehle [3,a], Miguel D. Mahecha [1,2,4], Yan Cheng [5], Henrik Hartmann [6,7,8], David Montero [1,4], Samuli Junttila [9], Stéphanie Horion [5], Mirela Beloiu Schwenke [10], Michael J. Koontz [11], Khairul Nizam Abdul Maulud [12], Stephen Adu-Bredu [13], Djamil Al-Halbouni [1], Muhammad Ali [14], Matthew Allen [15], Jan Altman [16,17], Lot Amorós [18], Claudia Angiolini [19], Rasmus Astrup [20], Hassan Awada [21,22], Caterina Barrasso [2,23], Harm Bartholomeus [24], Pieter S.A. Beck [25], Aurora Bozzini [26], Joshua Braun-Wimmer [14], Benjamin Brede [27], Fabio Marcelo Breunig [28], Stefano Brugnaro [29], Allan Buras [30], Vicente Burchard-Levine [31], Jesús Julio Camarero [32], Anna Candotti [33], Luka Capuder [34], Erik Carrieri [35], Mauro Centritto [36], Gherardo Chirici [37], Myriam Cloutier [38], Dhemerson Conciani [39], KC Cushman [40], James W. Dalling [41], Phuong D. Dao [42], Jan Dempewolf [43], Martin Denter [44], Marcel Dogotari [45], Ricardo Díaz-Delgado [46], Simon Ecke [14,43], Jana Eichel [47], Anette Eltner [48], André Fabbri [36], Maximilian Fabi [3], Fabian Fassnacht [49], Matheus Pinheiro Ferreira [50], Fabian Jörg Fischer [30,51], Julian Frey [14], Annett Frick [52], Jose Fuentes [53], Selina Ganz [3,54], Matteo Garbarino [35], Milton García [55], Matthias Gassilloud [3], Antonio Gazol [32], Guillermo Gea-Izquierdo [56], Kilian Gerberding [3], Marziye Ghasemi [57], Francesca Giannetti [37], Jeffrey Gillan [58], Roy Gonzalez [59], Carl Gosper [60], Terry Greene [61], Konrad Greinwald [62], Stuart Grieve [63,64], André Große-Stoltenberg [45,65], Jesus Aguirre Gutierrez [66,67], Anna Göritz [3], Peter Hajek [62], David Hedding [68], Jan Hempel [1], Stien Heremans [69], Melvin Hernández [55], Marco Heurich [70,71,62], Eija Honkavaara [73], Bernhard Höfle [74,75], Robert Jackisch [76], Tommaso Jucker [51], Jesse M. Kalwij [77,78], Sebastian Kepfer-Rojas [5], Pratima Khatri-Chhetri [79], Till Kleinebecker [45,65], Hans-Joachim Klemmt [43], Tomáš Klouček [80], Niko Koivumäki [73], Nagesh Kolagani [81], Jan Komárek [80], Kirill Korznikov [16], Bartłomiej Kraszewski [82], Stefan Kruse [83], Robert Krüger [48], Helga Kuechly [84], Ivan H.Y. Kwong [85], Etienne Laliberté [38], Liam Langan [86], Hooman Latifi [57], Claudia Leal-Medina [3], Jan R.K. Lehmann [87], Linyuan Li [88], Emily Lines [15], Maciej Lisiewicz [82], Javier Lopatin [89,90,91], Arko Lucieer [92], Antonia Ludwig [1], Marvin Ludwig [87], Päivi Lyytikäinen-Saarenmaa [73], Qin Ma [93], Nicolas Mansuy [94], José Manuel Peña [95], Giovanni Marino [36], Michael Maroschek [96,30], M.Pilar Martín [31], Darío Martín-Benito [56], Pavan Matham [81], Sabrina Mazzoni [36], Fabio Meloni [35], Annette Menzel [30], Hanna Meyer [87], Mojdeh Miraki [97], Gerardo Moreno [98], Daniel Moreno-Fernández [99,56], Helene C. Muller-Landau [55], Mirko Mälicke [100,101], Jakobus Möhring [1], Jana Müllerova [102], Setti Sridhara Naidu [81], Davide Nardi [26], Paul Neumeier [1], Mihai Daniel Nita [103], Roope Näsi [73], Lars Oppgenoorth [104], Sagynbek Orunbaev [72], Melanie Palmer [105], Thomas Paul [106],

* Corresponding author at: Institute for Earth System Science and Remote Sensing, Leipzig University, Germany.
E-mail addresses: clemens.mosig@uni-leipzig.de (C. Mosig), janusch.jehle@geosense.uni-freiburg.de (J. Vajna-Jehle).
[a] Shared first authorship.

https://doi.org/10.1016/j.rse.2025.115027
Received 12 February 2025; Received in revised form 29 August 2025; Accepted 12 September 2025
Available online 24 October 2025
0034-4257/© 2025 The Authors. Published by Elsevier Inc. This is an open access article under the CC BY license (http://creativecommons.org/licenses/by/4.0/).

Mattis Pfenning [3], Alastair Potts [107], Gudala Laxmi Prasanna [81], Suzanne Prober [108], Stefano Puliti [20], Antonio J. Pérez-Luque [56], Oscar Pérez-Priego [109], Chris Reudenbach [104], Jesús Revuelto [32], Gonzalo Rivas-Torres [110,4], Philippe Roberge [111], Pier Paolo Roggero [21,112], Christian Rossi [113], Nadine Katrin Ruehr [114], Paloma Ruiz-Benito [99], Christian Mestre Runge [104], Gabriele Giuseppe Antonio Satta [21], Bruno Scanu [21], Michael Scherer-Lorenzen [62], Felix Schiefer [77], Christopher Schiller [49], Jacob Schladebach [83], Marie-Therese Schmehl [115], Jonathan Schmid [3], Tristan Alexander Schmidt [3], Selina Schwarz [114], Rupert Seidl [30,96], Thomas Seifert [14], Ana Seifert Barba [34], Elham Shafeian [116], Aurélie Shapiro [117], Leopoldo de Simone [118], Hormoz Sohrabi [97], Salim Soltani [3], Laura Sotomayor [92], Ben Sparrow [119,120], Benjamin S.C. Steer [105], Matt Stenson [108], Benjamin Stöckigt [52], Yanjun Su [121], Juha Suomalainen [73], Elisa Tamudo [32], Mauro J. Tognetti Barbieri [122], Enrico Tomelleri [33,123], Michele Torresani [33], Katerina Trepekli [124], Saif Ullah [125], Sami Ullah [126], Josefine Umlauft [2], Nicolás Vargas-Ramírez [127], Can Vatandaslar [128,129], Vladimir Visacki [130], Michele Volpi [131], Vicente Vásquez [132], Christine Wallis [76], Ben Weinstein [132], Hannah Weiser [74,75], Serge Wich [133], Tagle Casapia Ximena [24,134], Pablo J. Zarco-Tejada [135], Katherine Zdunic [60], Katarzyna Zielewska-Büttner [136], Raquel Alves de Oliveira [73], Liz van Wagtendonk [79], Vincent von Dosky [137], Teja Kattenborn [3]

[1] *Institute for Earth System Science and Remote Sensing, Leipzig University, Germany*
[2] *Earth and Environmental Sciences Group, Center for Scalable Data Analytics and Artificial Intelligence (ScaDS.AI), Germany*
[3] *Chair of Sensor-based Geoinformatics (geosense), University of Freiburg, Germany*
[4] *German Center for Integrative Biodiversity Research (iDiv), Germany*
[5] *Department of Geosciences and Natural Resource Management, University of Copenhagen, Denmark*
[6] *Institute for Forest Protection, Julius Kühn Institute (JKI) - Federal Research Centre for Cultivated Plants, Germany*
[7] *Faculty of Forest sciences and Forest Ecology, Georg-August-University Göttingen, Germany*
[8] *Department of Biogeochemical Processes, Max Planck Institute for Biogeochemistry, Germany*
[9] *School of Forest Sciences, University of Eastern Finland, Finland*
[10] *Department of Environmental Systems Sciences, ETH Zurich, Switzerland*
[11] *Fort Collins Science Center, United States Geological Survey, United States*
[12] *Department of Civil Engineering, Universiti Kebangsaan Malaysia, Malaysia*
[13] *CSIR-Forestry Research Institute of Ghana, Ghana*
[14] *Chair of Forest Growth and Dendroecology, University of Freiburg, Germany*
[15] *Department of Geography, University of Cambridge, United Kingdom*
[16] *Department of Functional Ecology, Institute of Botany of the Czech Academy of Sciences, Czechia*
[17] *Faculty of Forestry and Wood Sciences, Czech University of Life Sciences, Czechia*
[18] *Dronecoria, Spain*
[19] *National Biodiversity Future Center (NBFC), Italy*
[20] *Norwegian Institute of Bioeconomy Research (NIBIO), Norway*
[21] *Department of Agricultural Sciences, University of Sassari, Italy*
[22] *National Biodiversity Future Centre, Italy*
[23] *Chair of Computational Landscape Ecology, Dresden University of Technology (TUD), Germany*
[24] *Laboratory for Geo-Information Science and Remote Sensing, Wageningen University, Netherlands*
[25] *Joint Research Centre, Ispra, European Commission, Italy*
[26] *Department of Agronomy, Food, Natural resources, Animals and Environment, University of Padua, Italy*
[27] *Section 1.4 Remote Sensing and Geoinformatics, GFZ German Research Centre for Geosciences, Germany*
[28] *Departament of Geography (DGEOG), Federal University of Paraná (UFPR), Brazil*
[29] *Geologist Flight Instructor and Remote Sensing, Italy*
[30] *TUM School of Life Sciences, Technical University of Munich, Germany*
[31] *Environmental Remote Sensing and Spectroscopy Laboratory (SpecLab), Spanish National Research Council (CSIC), Spain*
[32] *Instituto Pirenaico de Ecología, Spanish National Research Council (CSIC), Spain*
[33] *Faculty of Agricultural, Environmental and Food science, Free University of Bozen-Bolzano, Italy*
[34] *Department of Forest Protection, Slovenian Forestry Institute, Slovenia*
[35] *University of Turin, Italy*
[36] *Institute for Sustainable Plant Protection, National Research Council (CNR), Italy*
[37] *GeoLAB Laboratory of Forest Geomatics, Department of Agriculture, Food, Environment and Forestry, University of Florence, Italy*
[38] *Département de sciences biologiques, Université de Montréal, Canada*
[39] *Amazon Environmental Research Institute, Brazil*
[40] *Environmental Sciences Division, Oak Ridge National Laboratory, United States*
[41] *University of Illinois, United States*
[42] *Department of Agricultural Biology, Colorado State University, United States*
[43] *Bavarian State Institute of Forestry, Germany*
[44] *Chair of Remote Sensing and Landscape Information Systems, University of Freiburg, Germany*
[45] *Institute for Landscape Ecology and Resources Management (ILR), Justus Liebig University Giessen, Germany*
[46] *Remote Sensing & GIS Lab. Estación Biológica de Doñana, Spanish National Research Council (CSIC), Spain*
[47] *Department of Physical Geography, Utrecht University, Netherlands*
[48] *Institute of Photogrammetry and Remote Sensing, Dresden University of Technology (TUD), Germany*
[49] *Institute of Geographical Sciences, Freie Universität Berlin, Germany*
[50] *Department of Forest Sciences, "Luiz de Queiroz" College of Agriculture, University of São Paulo (USP/ESALQ), Brazil*
[51] *School of Biological Sciences, University of Bristol, United Kingdom*
[52] *Luftbild Umwelt Planung GmbH (LUP), Germany*
[53] *Department of Geography, Universidad del Valle, Colombia*

[54] Department of Biometry and Informatics, Forest Research Institute (FVA), Germany
[55] Smithsonian Tropical Research Institute, Panama
[56] Institute of Forest Sciences (INIA-CSIC), Spanish National Research Council (CSIC), Spain
[57] Department of Photogrammetry and Remote Sensing, K. N. Toosi University of Technology, Iran
[58] University of Arizona, United States
[59] University of Tolima, Colombia
[60] Biodiversity and Conservation Science, Western Australian Department of Biodiversity, Conservation and Attractions, Australia
[61] Department of Conservation Te Papa Atawhai, New Zealand
[62] Chair of Wildlife Ecology and Wildlife Management, University of Freiburg, Germany
[63] School of Geography, Queen Mary University of London, United Kingdom
[64] Digital Environment Research Institute, Queen Mary University of London, United Kingdom
[65] Centre for International Development and Environmental Research (ZEU), Justus Liebig University Giessen, Germany
[66] Environmental Change Institute, School of Geography and the Environment, University of Oxford, University of Oxford, United Kingdom
[67] Leverhulme Centre for Nature Recovery, University of Oxford, United Kingdom
[68] Department of Geography, University of South Africa, South Africa
[69] Research Institute for Nature and Forest (INBO), Belgium
[70] Department of National Park Monitoring and Animal Management, Bavarian Forest National Park, Germany
[71] Inland Norway University of Applied Science, Norway
[72] Environmental Sustainability and Climate Science, American University Central Asia, Kyrgyz Republic
[73] Department of Remote Sensing and Photogrammetry, Finnish Geospatial Research Institute, National Land Survey of Finland, Finland
[74] 3DGeo Research Group, Institute of Geography, Heidelberg University, Germany
[75] Interdisciplinary Center for Scientific Computing (IWR), Heidelberg University, Germany
[76] Geoinformation in Environmental Planning, Technische Universität Berlin, Germany
[77] Institute of Geography and Geoecology, Karlsruhe Institute of Technology (KIT), Germany
[78] Centre for Ecological Genomics & Wildlife Conservation, Department of Zoology, University of Johannesburg, South Africa
[79] School of Environmental and Forest Sciences, University of Washington, United States
[80] Faculty of Environmental Sciences, Department of Spatial Sciences, Czech University of Life Sciences Prague, Czechia
[81] Watershed Support Services and Activities Network (WASSAN), India
[82] Department of Geomatics, Forest Research Institute, Poland
[83] Polar Terrestrial Environmental Systems, Alfred Wegener Institute, Germany
[84] World Wide Fund for Nature (WWF) Germany, Germany
[85] Department of Geography and Resource Management, The Chinese University of Hong Kong, Hong Kong
[86] Quantitative Biogeography, Senckenberg Biodiversity and Climate Research Centre (SBiK-F), Germany
[87] Institute of Landscape Ecology, University of Münster, Germany
[88] College of Forestry, Beijing Forestry University, China
[89] Facultad de Ingeniería y Ciencias, Universidad Adolfo Ibáñez, Chile
[90] Data Observatory Foundation, ANID Technology Center No. DO210001, Chile
[91] Center for Climate Resilience Research (CR)2, University of Chile, Chile
[92] School of Geography, Planning and Spatial Sciences, University of Tasmania, Australia
[93] School of Geography, Nanjing Normal University, China
[94] Natural Resources Canada, Canadian Forest Service, Canada
[95] Tech4Agro, Institute of Agricultural Sciences (ICA), Spanish National Research Council (CSIC), Spain
[96] Research and Monitoring, Nationalpark Berchtesgaden, Germany
[97] Department of Forest Science and Engineering, Tarbiat Modares University, Iran
[98] Forest Research Group, INDEHESA, University of Extremadura, Spain
[99] Departamento de Ciencias de la Vida, Universidad de Alcalá, Spain
[100] Institute for Water and Environment - Hydrology, Karlsruhe Institute of Technology (KIT), Germany
[101] hydrocode GmbH, Karlsruhe, Germany
[102] Faculty of Environment, Dept. of Geoinformatics, Jan Evangelista Purkyně University in Ústí n. L., Czechia
[103] Department of Forest Engineering, Forest Management Planning and Terrestrial Measurements, Transilvania University of Brasov, Romania
[104] Universität Marburg, Germany
[105] Data and Geospatial Intelligence, Scion Research, New Zealand
[106] Forest Ecology and Management, Scion Research, New Zealand
[107] Spekboom Restoration Research Group, Nelson Mandela University, South Africa
[108] Environment, Commonwealth Scientific and Industrial Research Organisation, Australia
[109] Department of Forestry Engineering, University of Cordoba, Spain
[110] Estación de Biodiversidad Tiputini, Universidad San Francisco de Quito, Ecuador
[111] Earth System Science, Stanford University, United States
[112] Desertification Research Centre (NRD), University of Sassari, Italy
[113] Swiss National Park, Switzerland
[114] KIT-Campus Alpin, Karlsruhe Institute of Technology (KIT), Germany
[115] Department of Hydrology and Climatology, Potsdam University, Germany
[116] Department of Soil Science, University of Saskatchewan, Canada
[117] Food & Agriculture Organisation (FAO), Italy
[118] Department of Life Sciences, University of Siena, Italy
[119] School of Biological Sciences, The University of Adelaide, Australia
[120] Terrestrial Ecosystem Research Network (TERN), Australia
[121] State Key Laboratory of Vegetation and Environmental Change, Institute of Botany, Chinese Academy of Sciences, China
[122] Vorttex AP, Spain
[123] Competence Centre for Mountain Innovation Ecosystems, Free University of Bozen-Bolzano, Italy
[124] Faculty of Geology and Geoenvironment, National and Kapodistrian University of Athens, Greece
[125] State Key Laboratory of Desert and Oasis, Xinjiang Institute of Ecology and Geography, Chinese Academy of Sciences, Urumqi 830011, China
[126] Department of Forestry and Range Management, University of Kohsar, Pakistan
[127] Center for Multidisciplinary Research on Chiapas and the Southern Border, National Autonomous University of Mexico, Mexico
[128] Artvin Coruh University, Faculty of Forestry, Turkey
[129] Warnell School of Forestry and Natural Resources, University of Georgia (UGA), United States
[130] University of Novi Sad, Institute of Lowland Forestry and Environment (ILFE), Serbia
[131] Swiss Data Science Center, ETH Zurich and EPFL, Switzerland
[132] School of Forestry, Fisheries and Geomatics, University of Florida, United States

[133] School of Biological and Environmental Sciences, Liverpool John Moores University, United Kingdom
[134] Forest Program, Instituto de Investigaciones de la Amazonia Peruana (IIAP), Peru
[135] Institute for Sustainable Agriculture (IAS-CSIC), Spain
[136] Department of Forest Nature Conservation, Forest Research Institute (FVA), Germany
[137] unique land use GmbH, Germany

ARTICLE INFO

Edited by Jing M. Chen

Keywords:
Orthophoto
Drone
Tree mortality
Remote sensing
Database
Citizen science
Forests
Open-access

ABSTRACT

Excessive tree mortality is a global concern and remains poorly understood as it is a complex phenomenon. We lack global and temporally continuous coverage on tree mortality data. Ground-based observations on tree mortality, *e.g.,* derived from national inventories, are very sparse, and may not be standardized or spatially explicit. Earth observation data, combined with supervised machine learning, offer a promising approach to map overstory tree mortality in a consistent manner over space and time. However, global-scale machine learning requires broad training data covering a wide range of environmental settings and forest types. Low altitude observation platforms (e.g., drones or airplanes) provide a cost-effective source of training data by capturing high-resolution orthophotos of overstory tree mortality events at centimeter-scale resolution. Here, we introduce deadtrees.earth, an open-access platform hosting more than two thousand centimeter-resolution orthophotos, covering more than 1,000,000 ha, of which more than 58,000 ha are manually annotated with live/dead tree classifications. This community-sourced and rigorously curated dataset can serve as a comprehensive reference dataset to uncover tree mortality patterns from local to global scales using space-based Earth observation data and machine learning models. This will provide the basis to attribute tree mortality patterns to environmental changes or project tree mortality dynamics to the future. The open nature of deadtrees.earth, together with its curation of high-quality, spatially representative, and ecologically diverse data will continuously increase our capacity to uncover and understand tree mortality dynamics.

1. Introduction

In recent decades, elevated tree mortality rates have been reported for many regions of the world (Hartmann et al., 2022). This phenomenon is attributed to climate change-induced more frequent and intense climate extremes such as droughts, heatwaves, and late frosts, that often trigger outbreaks of damaging insects or epidemic diseases (Hartmann et al., 2022; Trumbore et al., 2015; Senf et al., 2020; Anderegg et al., 2013; Gora and Esquivel-Muelbert, 2021; Bauman et al., 2022; Hartmann et al., 2025). Tree mortality is generally not driven by a single driver but by complex compound events, consisting of multiple biotic and abiotic agents and feedbacks (Bastos et al., 2023; Mahecha et al., 2024; Allen et al., 2010; Schiefer et al., 2024). This may include a combination of consecutive heatwaves, meteorological and soil droughts, followed by late frosts after leaf budding, and the infestation of already weakened trees by pest and pathogens (Trugman et al., 2021; Stephenson et al., 2019; Fettig et al., 2019; Coleman et al., 2018).

Trees are long-lived and sessile organisms that cannot escape extreme conditions via migration, and their capacity to acclimate or adapt evolutionary to rapid environmental changes is low (Allen et al., 2015). Accordingly, the spatio-temporal patterns of standing dead tree canopies are direct indicators of how different tree species, functional types, ages, or entire ecosystems cope with biotic and abiotic stressors (Hartmann et al., 2022; Anderegg et al., 2013). Moreover, timely information on tree mortality dynamics is urgently needed by decision-makers in forest management and nature conservation. Information on tree mortality patterns is required to identify adaptation strategies, including selecting tree species, optimizing harvesting cycle, managing pest and disease outbreaks (*e.g.,* bark beetle), ensuring the provision of ecosystem services and controlling fuel accumulation for wildfire risk reduction (Stephens et al., 2018, 2022; Moghaddas et al., 2018; Vilanova et al., 2023; Garrity et al., 2013; Winter et al., 2024). Lastly, tracking tree mortality patterns helps indicate where ecosystems are undergoing rapid compositional transformations, *i.e.,* shift in species and their role in the terrestrial carbon cycle, *e.g.,* via declining net carbon sinks (Hill et al., 2023; Scheffer et al., 2001; Stephens et al., 2022; Pan et al., 2011; Migliavacca et al., 2025).

Despite its importance, the extent and rate of tree mortality at the global scale remains largely unknown or imprecise (Allen et al., 2015). Although ground-based inventories are the gold standard in forestry, national forest inventories only sometimes record tree mortality and are limited by sparse spatial coverage (Puletti et al., 2019) and low temporal sampling frequencies (*e.g.,* 10-year intervals), which do not align well with the rapid dynamics of environmental stressors (International Tree Mortality Network et al., 2025). Therefore, these inventories provide limited assistance in attributing tree mortality to short-term environmental dynamics such as climate extremes or insect outbreaks (Woodall et al., 2005; Hülsmann et al., 2017). Consequently, meta-analyses based on such ground observations could be biased or underrepresented for recent elevated tree mortality (Yan et al., 2024; Hammond et al., 2022). The value of field inventories for global tree mortality studies is further complicated by the commonly low data accessibility and heterogeneity in sampling protocols and data quality (McRoberts et al., 2010; Senf et al., 2018). Recent initiatives such as the global tree mortality database (Hammond et al., 2022) have gathered and harmonized invaluable information towards a global assessment of tree mortality. However, they are still severely limited in their spatial and temporal coverage and are not based on a systematic assessment that would enable scaling to larger spatial scales (International Tree Mortality Network et al., 2025). Uncovering global tree mortality patterns requires a multi-faceted approach that complements the ground-based assessments.

Satellite-based Earth Observation offers a promising avenue for global forest monitoring (International Tree Mortality Network et al., 2025). While remote sensing is generally only observing forest overstory dynamics due to its birds-eye view, it provides seamless spatial coverage and consistent monitoring across time. Using spectral imagery from the Landsat satellite mission, Hansen et al. created the prominent global *forest loss* map, Global Forest Watch, by applying a decision tree classifier on time series of spectral metrics (Hansen et al., 2013). However, this approach reveals a binary classification of forest cover loss, not tree mortality, and is restricted to 30 m spatial resolution and thus cannot detect the often scattered patterns of tree mortality (Cheng et al., 2024; Espírito-Santo et al., 2014; Schiefer et al., 2024). Unsupervised approaches involving analysis without labeled reference data can reveal continuous forest responses using anomalies of vegetation indices, which are computed by combining multiple spectral bands for each pixel (Thonfeld et al., 2022; Lange et al., 2024; Senf et al., 2018, 2020; Senf and Seidl, 2021). However, dynamics in vegetation indices reflect a wide range of vegetation changes and do not explicitly

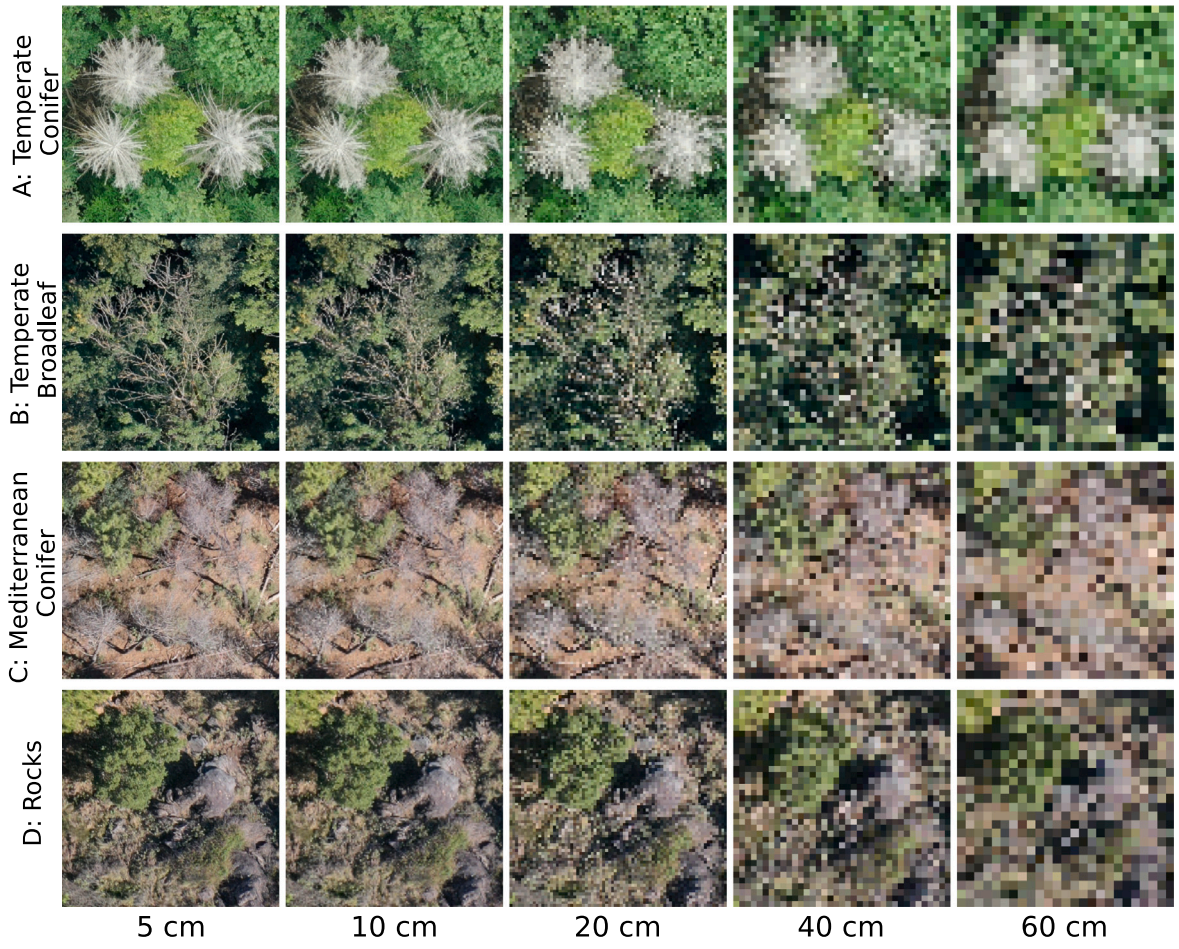


Fig. 1. Four forest sites, 15 m in width and height and at resolutions of 5 cm to 60 cm. From top to bottom (*A* to *C*), the tree species are *Picea abies*, *Fraxinus excelsior*, and *Pinus sylvestris*. Row *D* shows an example where rocks cannot be distinguished from standing deadwood in coarse-resolution images. The original images have resolutions better than 5 cm and were resampled (nearest-neighbor) for this visualization. Airplane images at the same resolution commonly appear less clear at similar resolutions, hence these images are best-case scenarios.

reveal tree mortality (Zeng et al., 2022). Therefore, translating the complex Earth observation signals to tree mortality patterns requires a supervised approach (Schiefer et al., 2023).

The Earth observation community, thus, currently lacks a representative collection of standardized reference data for training and validating supervised methods for monitoring tree mortality (Mansuy et al., 2024; Zhang et al., 2025). Given the relatively coarse resolution, satellite data does not provide the necessary spatial detail to extract such reference data directly. Ground observations are currently insufficient as reference data, primarily because they provide only point-based measurements that are constrained by limited positional accuracy (Leitão et al., 2018; Purfürst, 2022a; Kattenborn et al., 2021; International Tree Mortality Network et al., 2025). Airplane aerial images typically have higher resolutions and are often freely available for regions or entire countries and, therefore, provide a promising source to map tree mortality (Cheng et al., 2024; Junttila et al., 2024; Schwarz et al., 2024; Khatri-Chhetri et al., 2024). Photo-interpretation of such aerial images has a long tradition in forestry and has been used in this way operationally for decades. However, airplane imagery are only openly available in a few countries and their spatial resolutions typically range from 20–60 cm (*e.g.,* PNOA, Spain at 28 cm, NAIP, USA at 60 cm), in rare cases up to 10 cm (*e.g.,* swisstopo, Switzerland at 10 to 25 cm). This can be a critical constraint to uncover tree mortality, as an image resolution of 20 cm or less does not always enable most precise differentiation of dead from alive tree crowns and may lead to missing small dead trees (compare Fig. 1). For some species, crown shapes, or sizes, mortality is still clearly visible at 60 cm and in studies that are limited to specific ecosystems, *e.g.,* with dominantly coniferous species, coarse aerial images suffice (Junttila et al., 2024). Such resolution does not suffice, to accurately reveal partial dieback of broadleaf trees (row *B* in Fig. 1), mortality atop a bright forest floor (row *C* in Fig. 1), or in the presence of objects such as rocks that have a geometry that is similar to tree crowns (*e.g.,* rocks, row *D* in Fig. 1). Hence, to achieve accurate reference data across all ecosystems and tree types a finer resolution in the centimeter range ($\leq$10 cm) is needed, calling for a representative global collection of centimeter-scale imagery.

Drones are becoming increasingly accessible and user-friendly (Tang and Shao, 2015; Johnson et al., 2017; Rossi and Wiesmann, 2024). Suitable orthophotos for precise tree mortality identification at the centimeter scale can be obtained by non-technical users with consumer-type drones and easy-to-use mapping apps. Drones can safely fly over areas with dense understory or steep terrain without requiring physical access to the surveyed region. In a recent case study in Germany, Schiefer et al. (2023) exemplified the value of such high-resolution drone aerial images as reference to infer the fractional cover of standing deadwood [%] in pixels of satellite data (Sentinel-1 and -2). However, drones require operators to go into the field, creating significant labor costs and logistics challenges, especially if ground control targets are needed. Hence, leveraging drone orthophotos for use in global tree mortality monitoring can only be achieved through a large collective effort across institutions, researchers, and citizens across the globe, to finally acquire a rich collection of orthophotos to represent all forest ecosystems.

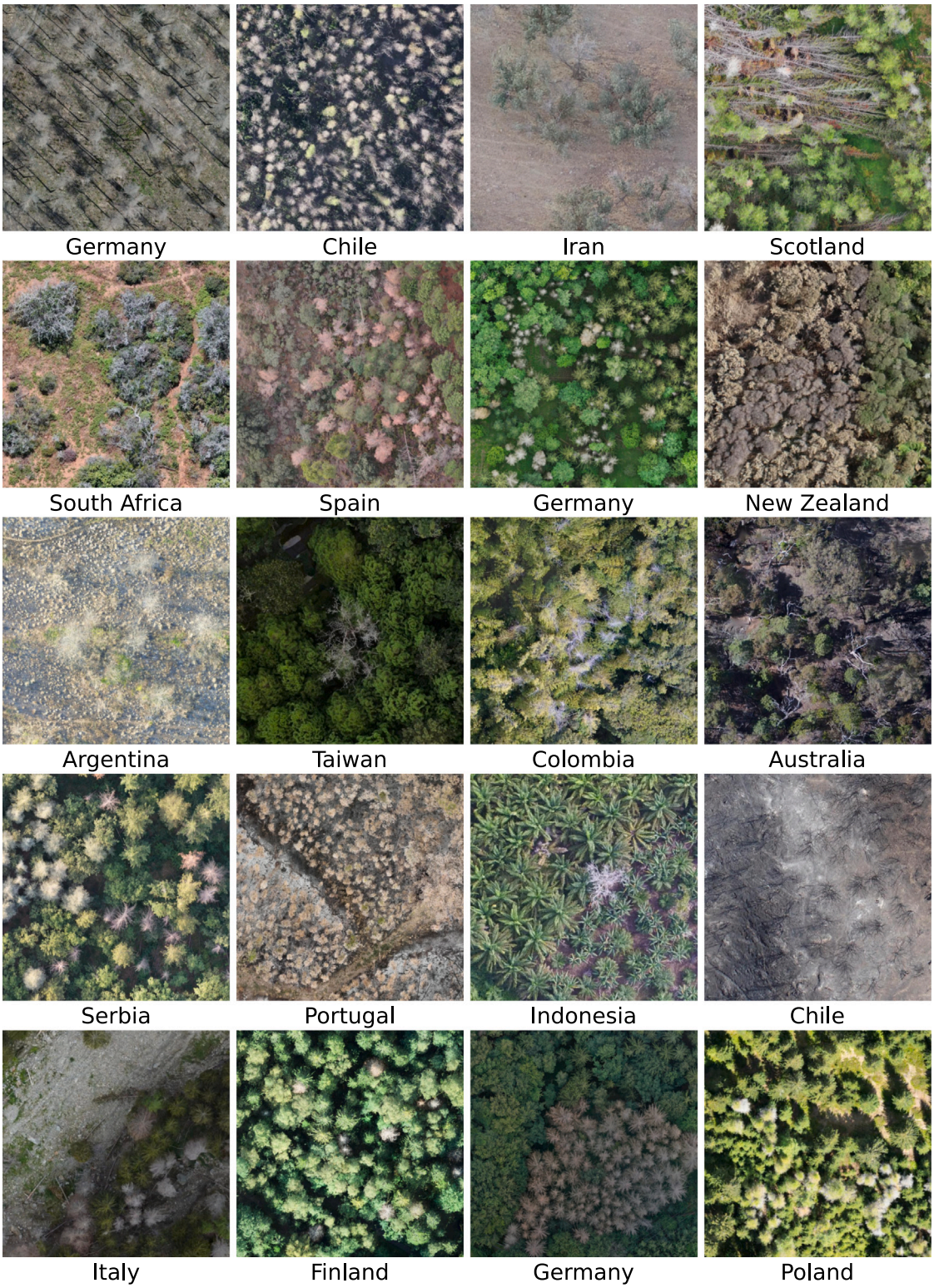


Fig. 2. Sample image sections of standing deadwood in a variety of contexts. The caption below each image denotes the acquisition location of the drone orthophoto. All images are available in the database. (For interpretation of the references to color in this figure legend, the reader is referred to the web version of this article.)

Here, we introduce deadtrees.earth, an open science, collaborative platform for accessing, sharing, analyzing, and visualizing a global database of orthophotos with labeled standing deadwood. The deadtrees.earth platform features open-access interactive functionality, allowing users to upload and download images and labels through the website and an API. It also incorporates expert quality control workflows to maintain high data standards. This collection, across spatial and temporal scales, offers unparalleled opportunities for researchers to advance satellite-based model training and validation. The platform's backend is built with a scalable architecture to allow growth into a

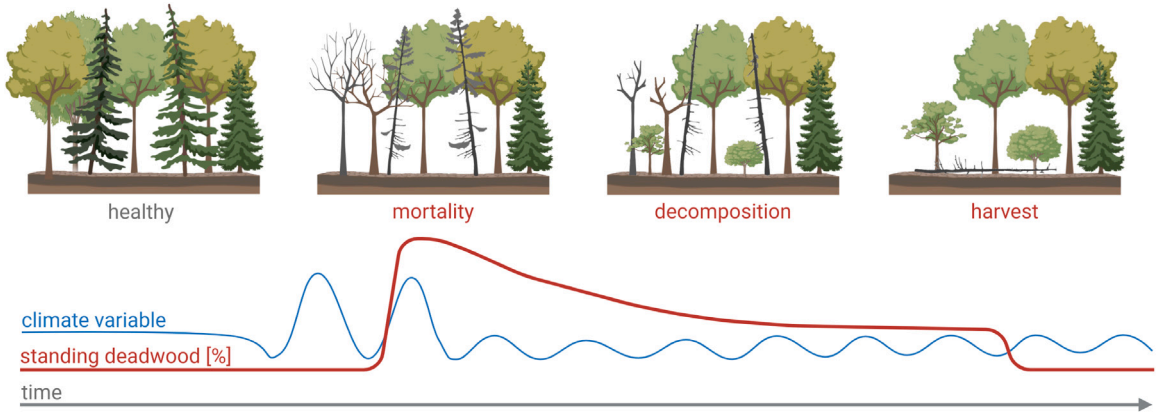


Fig. 3. Temporal signature of standing deadwood (red) in multiple scenarios. Climate extreme events (blue) cause tree mortality to increase. Natural decomposition and/or salvage logging decreases standing deadwood. (For interpretation of the references to color in this figure legend, the reader is referred to the web version of this article.)

large machine learning model ecosystem. Beyond machine-learning applications, this database also enables verification of existing products. Contributors are acknowledged for their data contributions, fostering transparent community participation and acknowledgment.

2. The deadtrees.earth platform

deadtrees.earth is a dynamic, community-built, open-access database for aerial orthophotos of delineated standing deadwood. This section presents our definition of standing deadwood, the database structure, database statistics, and a web platform for the integration of the database into the community.

2.1. Standing deadwood

We focus on *standing deadwood*, defined as woody material (twigs, branches, or stems) in the upper canopy layer that has died off but has largely retained its original structure. Both evergreen and deciduous dead tree canopies are visually identified by either leaves or needles in a gray or brown state or a lack of foliage (Fig. 2). While evergreen trees can be detected in any season, for deciduous trees it is required to only consider imagery in leaf-on season, *i.e.,* summer or wet season. Standing deadwood can be identified in centimeter-scale RGB images acquired by drones or airplanes by methods such as semantic segmentation, which involves the generic segmentation of any dead tree crown or branch (Schiefer et al., 2023; Möhring et al., 2025), or instance segmentation, where each segment corresponds to an individual tree crown (Cheng et al., 2024).

Information on lying deadwood is not considered for this database. In contrast to standing dead tree crowns, fallen tree stems are less likely to be detected in drone and airplane imagery, as they are readily occluded by surrounding tree crowns or are rapidly covered by understory. Additionally, fallen trees can be several decades old and are hence less interesting for studying tree mortality as a response to recent environmental changes, climate extremes, or pests and pathogens.

The amount of standing deadwood changes over time with different events (Fig. 3). Climate extreme events, such as droughts, can cause tree mortality, increasing the amount of standing deadwood. Standing deadwood is not limited to fully dying trees; partial dieback also affects the amount of standing deadwood. Explicitly including partial dieback is important, as it is an important measure for ecosystem resilience and a key indicator for forest condition surveys. In subsequent years, the dead tree crowns decompose and the fraction of standing deadwood decreases. As soon as dead trees fall over, are felled, or are completely removed, they no longer count as standing deadwood.

Although the concept of standing deadwood is simple, understanding its temporal dynamics requires several considerations. First, the disappearance of healthy trees does not affect the fraction of standing deadwood. This also includes removing unhealthy trees that have not yet changed their appearance from above and are removed before visible leaf loss. Secondly, the amount of standing deadwood does not contain information about the year of death. Note that the year of the first appearance can be extracted from a standing deadwood time series (Schiefer et al., 2024). Thirdly, drought or cold semi-deciduous species that shed their leaves during climate extremes or species that resprout epicormically after disturbances such as fire, may visually appear as standing deadwood at one point in time but may regrow leaves at a later time, *e.g.,* red needle cast (Watt et al., 2024) or drought-induced leaf shedding (Gentilesca et al., 2017).

2.2. Database structure

The deadtrees.earth database is a collection of geo-referenced RGB orthophotos with optionally one or more sets of labels depicting standing deadwood. Our database focuses on airborne imagery with resolutions finer than 10 cm while also allowing submissions of lower resolutions for unrepresented regions, where validated tree mortality labels are provided, or standing deadwood can be clearly identified (Fig. 1).

Each **orthophoto** comes with the following metadata: acquisition date, author(s), platform, resolution, greenness phenology curve, and license (compare Fig. 4). The author can be one or multiple individuals who contributed to capturing the orthophoto.

The acquisition date is crucial for linking with environmental conditions to validate whether the orthophoto was captured in leaf-on season because one cannot differentiate between dead and alive trees in orthophotos that were captured in leaf-off season. Given that data contributors track the acquisition date with different accuracy, we accommodate three levels of precision for the acquisition date, that is, accurate in days, months, or years. Noting the possible temporal error is of utmost importance when combining these observations with other datasets, such as satellite time series (see Section 3.2).

Local information on canopy greenness phenology at the ecosystem scale is derived from the VIIRS Global Land Surface Phenology Product (Zhang et al., 2020). The VIIRS product reports up to two periods of 'Maximum Greenness' based on the Enhanced Vegetation Index. This period is defined as between the 'maturity onset or end of spring' and the 'senescence onset or start of fall'. Acquisitions within that period are most likely to be leaf-on. Observations outside this period are not necessarily in leaf-off season. The probability distribution for each day-of-year to be in this period is provided to users as additional

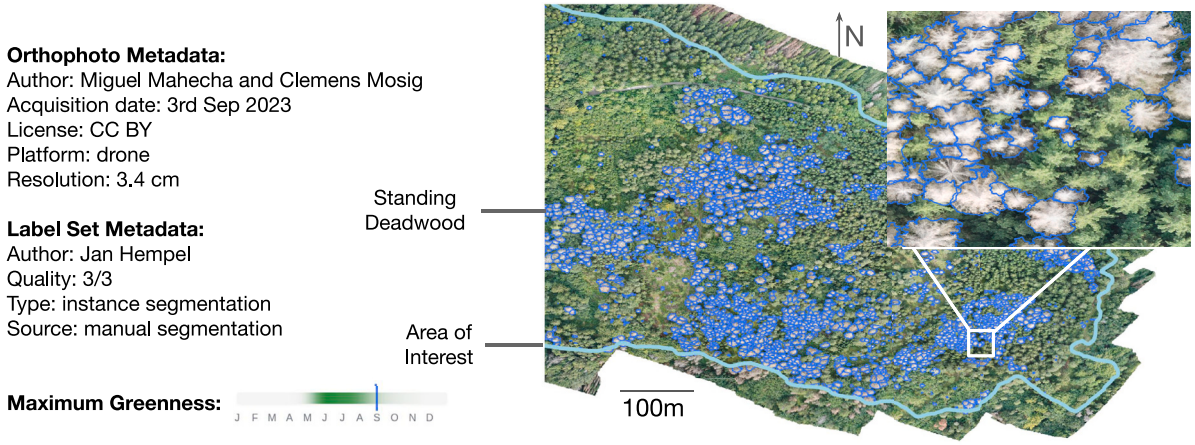


Fig. 4. Sample entry of an orthophoto(ID=306) (Jena, Germany, centroid: 50.911271°N 11.509977°E) with one label set for one area of interest (AOI) in the deadtrees.earth database. Only a simplified set of attributes are shown, see Figure 8 in Supplementary material for the precise database structure.

metadata (see Subsection 5.2 in Supplementary material). In some ecosystems this proxy should be interpreted with great care. Pixel-level heterogeneity, can bias the inferred leaf-on period, particularly where summer- and winter-deciduous trees co-occur within a pixel or herbaceous groundcover influences the signal under sparse canopies (Zhang et al., 2018). Therefore, this product primarily serves as an indicator. In the future, higher-resolution phenology products, *e.g.,* based on Sentinel-2, PlanetScope, are expected to reduce these issues.

For each orthophoto, the average ground sampling distance (GSD) is automatically calculated to allow users to filter data based on different spatial resolutions (see Fig. 4). Orthophotos can be submitted using established coordinate reference system and are stored accordingly. Reprojection is only performed for coherent visualization on the website. Finally, the location quality of a submitted orthophoto is visually assessed by the project team using open aerial map services to compare conspicuous features. Orthophotos with a more than 15 m shift are discarded.

Regardless of the spatial resolution, the information quality of an orthophoto can be constrained by various factors. These constraints include poor lighting conditions (*e.g.,* underexposure), reconstruction artifacts, motion blur, or data gaps (Dandois et al., 2015; Frey et al., 2018). The image condition can vary heavily across an orthophoto, *e.g.,* image edges are often distorted. The non-distorted parts of the orthophoto may still not represent the true appearance of the forest and small-scale mortality can be missed in the stitching process in rare cases (Koontz et al., 2021). To account for such variance within orthoimages, we assign each orthophoto an **area of interest (AOI)**, a multi-polygon the delineates the part of the orthophoto where tree mortality can be clearly identified and the image is not distorted. The AOI is determined during a meticulous manual audit by data stewards of the deadtrees.earth platform, provided for each dataset for download and visualized for each individual aerial image submission under https://deadtrees.earth/dataset.

Label sets are polygons or points located over standing deadwood in orthophotos identified through visual inspection or from automatic segmentation (Schiefer et al., 2023; Cheng et al., 2024; Junttila et al., 2024). More specifically, there are four types of labels: (*i*) centroids of individual dead tree crowns, (*ii*) bounding boxes of individual dead trees, (*iii*) delineations of individual dead tree crowns (instance segmentation), and (*iv*) delineations around a group of adjacent dead trees or dead tree parts (semantic segmentation). Each label set is associated with an AOI, that also acts as boundary of the labeling effort. This means area inside the AOI that was not marked as deadwood can be assumed to be alive or non-tree objects (see Fig. 4). Lastly, there can be multiple sets of labels from different sources for the same orthophoto, *e.g.,* one may have been created manually while a second set was machine-generated by a segmentation model.

The quality of the labels will be assessed during an audit, where, again, a quality score between 1 and 3 will be assigned. A score of 3/3 means accurately delineated standing deadwood and partial dieback (see Fig. 4). In the score of 2/3 we include sets where the vast majority of deadwood is labeled and/or delineations have imperfections, *e.g.,* partially include forest floor or disregard partial dieback. Label sets with a score 1/3 include all other sets and are recommended to be excluded in further analysis or machine learning applications.

2.3. Platform architecture

The deadtrees.earth platform is an integrated web-based system designed to facilitate visualization, participation, management, and access to the deadtrees.earth database. The platform architecture consists of the following components: a user-facing front-end application, a self-hosted database for metadata and labels, a Cloud-hosted storage server for orthophotos and Cloud Optimized GeoTIFFs (COGs), a processing server for generating COGs, and user authentication (see Fig. 5).

The front-end of the platform includes a landing page introducing users to the platform's features, and a dataset page for searching and filtering the database through a list or world map. Users can select a specific dataset to access the *details page*, which visualizes one orthophoto with corresponding labels and their metadata. From here, users can download datasets without needing an account. Each label set is uniquely linked to one orthophoto (N:1 schema), and this relationship is preserved during download: dataset IDs are shown to the user and embedded in filenames to ensure reliable traceability between imagery and labels. A second page visualizes large-scale satellite-based deadwood maps. Finally, a user-specific profile page, which requires login, enables users to upload orthophotos and labels and manage their data.

Registered users can upload orthophotos, in the form of GeoTIFFs, and labels to the system together with a set of metadata data that includes the author names and acquisition date per orthophoto. Upon successful submission to the system, additional metadata is generated, that is, administrative level, information about local phenology and technical image details. All metadata, along with vector labels, is stored in a self-hosted Supabase database, which is accessible via Python and JavaScript client libraries. Data audit workflows require specific user access levels, which are assigned to the deadtrees.earth core team. For user authentication, we use Supabase Auth, which is based on JavaScript Object Notation Web Tokens (JWTs). This ensures secure access while integrating with Supabase's database features to implement Row Level Security (RLS), ensuring that each user can only access

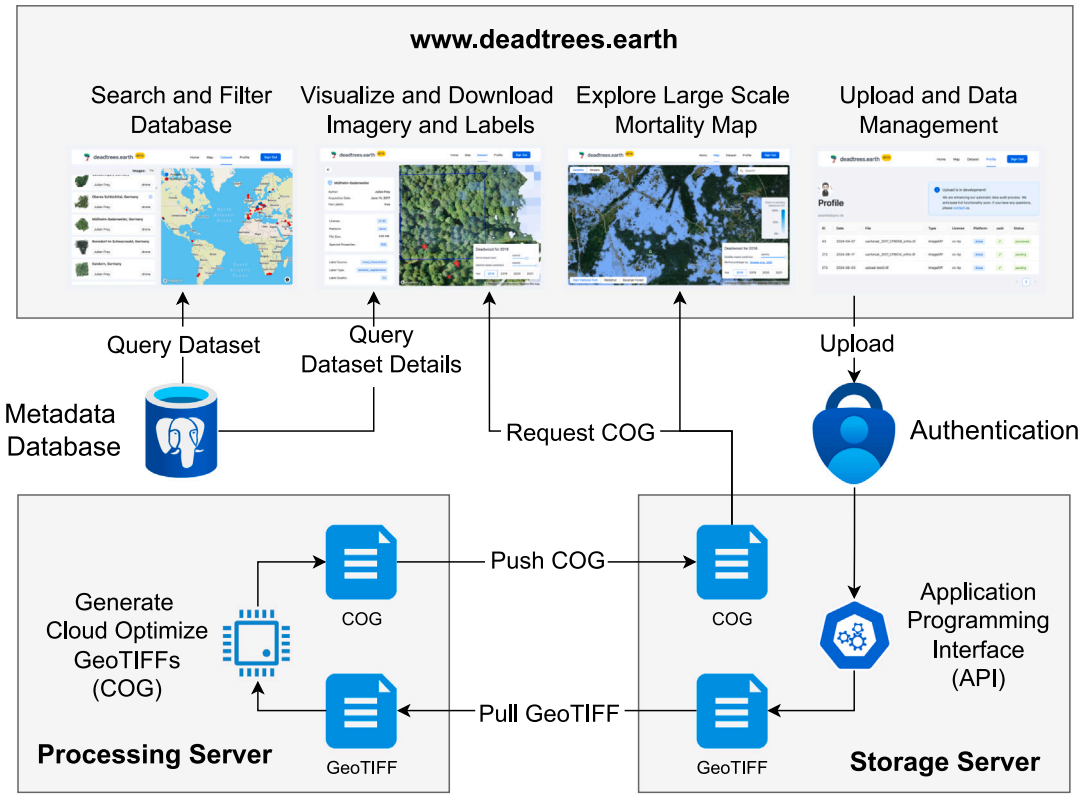


Fig. 5. System diagram illustrating the main components of the deadtrees.earth platform and their interactions. Users can search and filter the database, visualize and download orthophotos, and explore a large-scale mortality map. The processing server generates Cloud Optimized GeoTIFFs (COGs) by pulling GeoTIFF files and pushing processed COGs to the storage server.

data they are authorized to view. All critical components, including the storage server and Supabase database, are backed up daily using Borg (https://www.borgbackup.org/). Backups are stored offsite on a university-maintained file server at the University of Freiburg, integrated into the institutional backup strategy.

To efficiently visualize a large collection of orthophotos with minimal resources, the platform uses Cloud Optimized GeoTIFFs (COGs). COGs allow users to view and work with large orthophotos quickly and efficiently, which is especially helpful when bandwidth or processing power is limited. COGs are internally tiled and include overviews, making them accessible via HTTP range requests without the need for server-side processing. This approach allows clients to fetch only the necessary data, optimizing transfer and reducing server load. As a result, COGs significantly improve performance compared to traditional Web Map Services (WMS) such as GeoServer (https://geoserver.org/) or MapServer (https://mapserver.org/).

The resource-intensive generation of COGs is performed on a separate processing server. The server periodically pulls user-uploaded GeoTIFF files from the storage server, performs the necessary processing, and pushes the generated COGs back to the storage server (see Fig. 5).

A Python-based REST API (REpresentational State Transfer Application Programming Interface) built with FastAPI (https://fastapi.tiangolo.com/) manages upload/download workflows, processing tasks, user management, and resource allocation. While this API is not yet public, larger data requests can be fulfilled upon request, and full API access is a near-term development goal. The front-end initiates tasks such as uploading, downloading, metadata generation, and processing COGs through this REST API, which can also be used directly for programmatic data ingestion and processing. The deadtrees.earth API also employs a queuing system to manage processes and prevent downtime which ensures stability and scalability.

Finally, the platform's modular design allows for future integration of advanced workflows, such as machine learning models for automated deadwood segmentation from drone imagery. By leveraging powerful local processing servers, these workflows can be added seamlessly, making the platform adaptable and flexible to meet evolving needs.

2.4. Data sources and current state of the database

The primary sources for the orthophotos and labels are community contributions, *i.e.,* datasets that individuals or institutions actively contributed. Given the large interest in monitoring tree mortality dynamics worldwide, the deadtrees.earth database received tremendous support from a wide array of individuals and institutions. So far, 136 institutions shared data across 89 countries.

Crowd-Sourcing: In addition to community contributions, the database integrates crowd-sourced data, *i.e.,* datasets already freely available online. Indeed despite extensive community efforts to date, significant portions of the Earth remain uncovered in our database. Therefore to maximize database coverage, we integrate publicly available databases that adhere to appropriate licensing schemes.

While other initiatives, such as GeoNadir, OpenAerialMap, and OpenDroneMap, also collect drone orthophotos, only OpenAerialMap currently ensures that all contributions are licensed under CC BY (Creative Commons), making them suitable for use in projects like deadtrees.earth. As of June 2024, OpenAerialMap hosts over 15,000 aerial orthophotos. We use this community-driven resource to expand the deadtrees.earth database. However, most of the contributions to OpenAerialMap do not meet our database criteria due to limitations in resolution, site relevance, quality, or acquisition timing. To be able to extract usable images, we downloaded a summary of the metadata on 24th April 2024 through their open API. Then we first filter the entries where at least 30% is covered by forest according to ESA Worldcover (Zanaga et al., 2022). To then remove orthophotos that

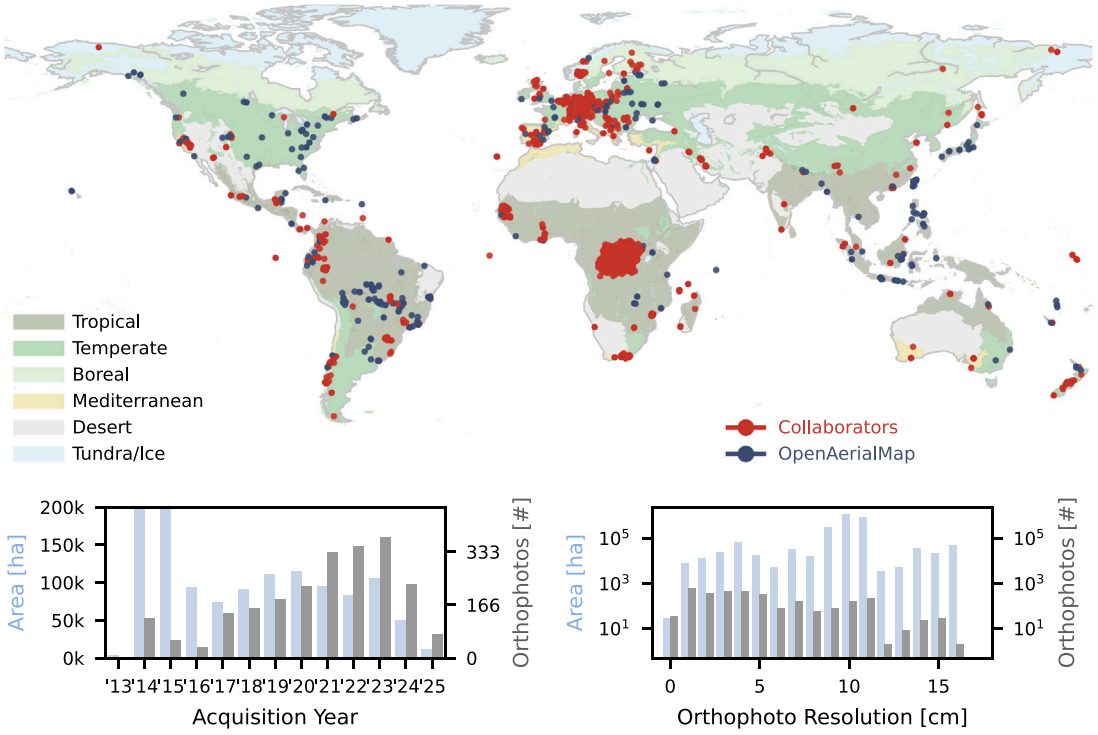


Fig. 6. Initial statistics of the database upon launch depicting geographical, temporal, and resolution diversity. In the two bottom panels, drone orthophotos are accumulated by area (light blue) and count (dark gray). Statistics are only shown for years with more than five orthophotos. Different colors in the background depict different biomes (Olson et al., 2001). (For interpretation of the references to color in this figure legend, the reader is referred to the web version of this article.)

lack the necessary spatial resolution (Fig. 1), we filtered images to include only resolutions finer than 10 cm, yielding 1102 samples. To only include orthophotos of forests within the growing season, we filtered the months May to August for samples north of latitude 23.5°N, December to March for samples south of latitude 23.5°S, and included all images for latitudes in between. Note that at a later stage we will differentiate between wet and dry seasons for tropical region. Finally, we manually iterated through the thumbnails to remove imagery with obvious quality issues and then assessed the original GeoTIFF. This resulted in a final set of 448 (out of >15,000 on OpenAerialMap) orthophotos with wide temporal (2007 to 2024) and geographic coverage (see Fig. 6).

It is worth noting that the dataset extracted from OpenAerialMap has a bias towards forests near human settlements, potentially overrepresenting ecosystems that might not be representative of the region. For example, an orthophoto may contain 20 ha of a relevant forest, but another 100 ha of the image contains a building site that the drone operator originally planned to capture. Nevertheless, this crowdsourced dataset provides valuable, high-resolution imagery of forests in ecosystems that would otherwise not be part of our database. Additionally, this bias may provide an opportunity for studies focusing on studying forest fragments and urban forests. As OpenAerialMap grows in the future, we will continuously monitor their database for relevant submissions. Also, other relevant sources with a CC-BY license or similar permissive licenses will be integrated.

Database Statistics: We launched the seed database with 2694 centimeter-scale orthophotos covering 1,033,1099 ha and spanning all continents (except Antarctica) through community contributions and crowd-sourced data. By the time of writing (Jul. 2025), the database consists of 2246 (83%) drone orthophotos from community contributions and 448 (17%) crowd-sourced orthophotos extracted from OpenAerialMap (Fig. 6). The increasing ease of use of drones within the last decade is reflected in the greater number of unique orthophotos in recent years. Additionally, the database includes 539 aerial images with resolutions less than 10 cm (Fig. 6).

Notable Collections: Although a large part of the database consists of individual locations that have been captured, it also features noteworthy collections that provide independent value, for example through temporal coverage across multiple months or years. Notable collections include:

- **Barro Colorado Island (Panama)** 90 orthophotos capturing the same 50 ha plot across 6 years (Vasquez et al., 2023).
- **Québec (Canada)** Seven consecutive orthophotos of the same lake area from May to October 2021 (Cloutier et al., 2023).
- **Sierra Nevada Mountain Range (California, United States)** 32 (>30 ha) plots distributed over a 350 km and 1000 m elevational gradient in dry mixed conifer forest of California. Imagery captures the aftermath of a mass tree mortality event arising from the 2012 to 2016 hot drought (Koontz et al., 2021).
- **Black Forest National Park (Germany)** A 10-year timeseries covering the entire national park (Christoph Dreiser).
- **Baden-Württemberg (Germany)** 135 unique plots (>1 ha) in southwest Germany captured in up to three different years, respectively (ConFoBi).
- **ECOSENSE (Germany)** A highly dense and continued time series at approximately monthly interval of the forest site of the ECOSENSE Collaborative Research Centre (3 ha) in southwest Germany (Werner et al., 2024).
- **Andalusia (Spain)** 60 tree mortality sites (>15 ha) in otherwise protected national parks in 2023 (Clemens Mosig and Oscar Pérez-Priego).
- **Eastern Cape (South Africa)** 35 tree mortality sites captured between 2022 and 2024 providing unique data from Africa (Alastair Potts).

- **Zagros forests (Iran)** 16 RGB Orthophotos captured in ca. 1 ha sample plots representing *Quercus brantii* Lindl. (Brant's oak) decline. Distributed over the large latitudinal gradient of semiarid Zagros Forests in western Iran (Ghasemi et al., 2022, 2024b,a).
- **Norwegian Institute of Bioeconomy Research archive (NIBIO, Norway)**: 50 orthophotos RGB orthophotos captured by NIBIO's Forest and Forest Resource division between 2017–2022 using a variety of DJI drones. These data were collected primarily in south eastern Norway (Puliti et al., 2020, 2019; Bhatnagar et al., 2022).
- **World Wildlife Fund (WWF) (Democratic Republic of the Congo)**: Orthophotos at 218 locations systematically sampled across closed-canopy forests in the Congo Basin in 2014. Comprehensive collection from the world's second largest tropical rainforest (Xu et al., 2017).

The latter eight collections have not been available to the public until now.

Labels: The database contains 54,320 *manually delineated* polygons delineating partial dieback, individual trees or multiple dead tree crowns. In total, 493 orthophotos and 58,219 ha are fully labeled, of which 245 label sets have quality *3/3*, 231 have quality *2/3*, and 5 have quality *1/3* (see Section 2.2 for quality definition). The manual label set covers all biomes, predominantly focusing on Temperate and Mediterranean biomes (Möhring et al., 2025). These datasets will soon be available as machine learning ready datasets (see Section Section 3) to support the community with training semantic or instance segmentation models. At present, this unique data collection would result in more than 600,000 labeled 512 × 512 patches or 170.000 labeled 1024 × 1024 patches.

For this data collection we strictly adhere to the FAIR principle (Wilkinson et al., 2016). All data is **F**indable, *i.e.,* has a unique identifier, is described with metadata, and thus searchable. **A**ccess is provided through industry-standard and authentication-free HTTP requests on the website or programmatically (see Section 2.3). We provide data **I**nteroperability by using GeoTIFF format and standard datatypes for metadata (see Figure 8 in Supplementary material). Lastly, all data is **R**eusable as it is published under a Creative Commons license.

In summary, through community efforts and crowd-sourcing of data, and to the best of our knowledge, the deadtrees.earth database curates an unprecedented amount of centimeter-resolution optical imagery and corresponding labels. With the increasing recognition of this database and the general growing willingness for open data in science and the public, we expect this database to continue expanding rapidly.

3. Outlook and perspective

3.1. Database expansion through community contribution

Excess tree mortality is a global phenomenon whose underlying complexity can only be effectively assessed through community effort (International Tree Mortality Network et al., 2025). The deadtrees.earth platform initiates with a collection of centimeter-scale forest orthophotos that is already orders of magnitude larger in spatial coverage and diversity than in any mortality-related study used. However, this collection is biased towards the Global North, and regions in Asia and Africa are particularly underrepresented (see Fig. 6). This presents an opportunity for future orthophoto contributions from additional geographic regions around the world, helping to establish a more representative collection of global tree mortality. We therefore encourage everyone in every community to take the opportunity to participate in this global initiative.

Newly submitted orthophotos of local tree mortality events bolster the global and temporal representativeness of the database. This is critical for training models that aim for a global transferability (Meyer and Pebesma, 2022; Kattenborn et al., 2022; Möhring et al., 2025), be it computer vision models that segment dead trees in drone data or satellite-based models. Hence, an individual submission of a user's local forest can be an important missing puzzle piece in creating a representative training dataset. Subsequently, machine-learning models will improve in the user's local region, providing a strong incentive to contribute their data as they indirectly benefit.

This platform is deliberately calling for RGB imagery only. While multispectral and hyperspectral sensors offer additional spectral bands, they typically come with lower spatial resolution and significant variability in band configurations and radiometric quality, making them less suitable for crowd-sourced applications. Additionally, drones equipped with such sensors are currently several times more expensive than consumer drones with RGB cameras. Low-cost consumer drones with RGB cameras are widely available and offer spectral homogeneity and centimeter-level spatial detail. Hence, to maximize participation, and thus the coverage of this database, we opted to focus only on RGB orthophotos.

3.2. Towards tree mortality models and products from local to global scale

Delineated standing deadwood identified from large amounts of centimeter-scale orthophotos is a powerful data source for creating high-precision training data. Deadtrees.earth provides a unique dataset that will enable the machine-learning community to create models and maps that are transferable at a global scale and robust across the diversity of forest ecosystems (Fig. 7).

Given the rich database presented here, users can train various types of **computer vision models for identifying standing deadwood in drone orthoimagery**, *e.g.,* in the form of semantic segmentation (polygons of dead crowns, twigs or branches), object detection (bounding boxes of individual trees), or instance segmentation (precise crowns of individual trees). One such example is Möhring et al. (2025), a globally generalizing semantic segmentation which was directly trained on this database. With such models, one can perform inference on all orthophotos in the database to automatically reveal the local distributions of standing deadwood. This is particularly relevant for orthophotos that do not have labels from a human interpreter. Machine-learning-based predictions may even be advantageous over labels from human interpreters as they might be more standardized and objective (in contrast to manually delineated polygons from different human interpreters). This automated mapping of standing deadwood is also meant to be one of the core incentives for users interacting with the deadtrees.earth. Thus, deadtrees.earth will provide a hub for making machine-learning-based technology developed by the community accessible for non-experts (*e.g.,* practitioners, citizens, non-government organizations) or people with limited resources.

The local patterns of overstory mortality derived from orthophotos can be used as a reference for **large-scale machine-learning-based mapping using satellite data** from Sentinel, Landsat, or future satellite missions (Schiefer et al., 2023). While Sentinel and Landsat data are much coarser in resolution than drone data, approximately 10 m to 30 m, respectively, they have the advantage of having global coverage and being multi-spectral data. The temporal continuity of Sentinel or Landsat data supports the creation of accurate global products, as machine-learning models can harness the temporal and spectral patterns. For example, in optical satellite imagery, standing deadwood may look visually similar to a grayish forest floor or rocks (Fig. 1). However, in a time series of multiple years, a dead tree can be differentiated from a forest floor or rocks based on its spectral history. For example, Schiefer et al. leveraged this approach to build a yearly, fractional tree mortality map for Germany based on an orthophoto dataset that makes up less than 1% of this database by area achieving an RMSE of 0.22 Pearson's R of 0.66. Building on this methodology, deadtrees.earth will provide satellite-based models and predictions at a global scale in the near future.

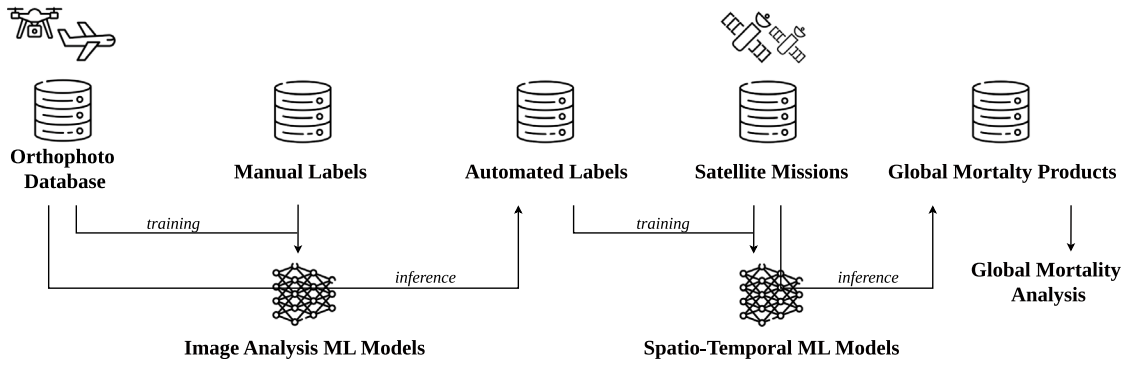


Fig. 7. Generalized workflow to derive a global tree mortality product through the deadtrees.earth database and machine learning (ML) models.

To stimulate the development of machine-learning models for analyzing drone and satellite data, deadtrees.earth will provide ML-ready datasets, *e.g.,* integrated into the torchgeo library (Stewart et al., 2022). This will enable the community to develop and benchmark different methods effectively. Incentives for this might be further propelled by related coding competitions. Moreover, the machine-learning-ready datasets will enable the development of workflows that are directly compatible with the deadtrees.earth ecosystem, so that models and workflows developed in the community can be directly integrated as an application.

With the launch of deadtrees.earth we aim to attract a variety of communities to this multifaceted platform. Through simple, interactive visualizations of orthophotos together with labels and satellite-derived products on the website, we truly enable anyone to explore our and others' tree mortality-related products. Viewing centimeter-scale imagery and satellite products side-by-side will enable benchmarks, validation, and finally an understanding of large-scale patterns of forest mortality. In a citizen science approach, non-specialists can also contribute data without prior knowledge of machine-learning methods used for further processing by us and the broad scientific community. In the future, we aim to further increase participation on deadtrees.earth by enabling users to delineate standing deadwood manually, correct AI segmentation outputs, and flag faulty predictions in the satellite data.

3.3. Combining aerial imagery with ground-based observations

While aerial imagery and machine-learning models enable scalable mapping of tree mortality, a critical next step is to link these observations with field data. Such a combination would not only provide a pathway for validating remote sensing products, but also enable new applications, for example by combining crown-level mortality maps with field-based biomass estimates to quantify carbon loss. However, this integration remains highly challenging (International Tree Mortality Network et al., 2025; Kattenborn et al., 2019). Ground-based surveys currently provide rather coarse plot-level information, not spatially explicit crown data (International Tree Mortality Network et al., 2025). Even when individual tree positions are recorded, they are typically mapped as stem points, which cannot be directly aligned with polygons of crowns in aerial imagery (Schiefer et al., 2023). This mismatch is further amplified by GNSS errors, which commonly range from 3–5 m and may exceed 10 m under dense canopies (Valbuena et al., 2010; Kaartinen et al., 2015; Purfürst, 2022b), far beyond the location accuracy and centimeter-scale resolution that can be achieved with drone imagery (Hugenholtz et al., 2016). Moreover, tree crowns are rarely centered above stems, often have irregular shapes, and are difficult to observe from below due to canopy occlusion. As a result, both complete mortality (whole crowns) and partial dieback (branches or crown sectors) are very likely to be underestimated in ground surveys (Kattenborn et al., 2021; Schiefer et al., 2023). In addition, field surveys are typically very resource intensive, and in combination with sampling uncertainties and the above-described measurement limitations, they may hardly suffice to serve as validation for remote sensing products at global scales.

Looking forward, a systematic strategy is required to overcome these challenges and enable robust integration of aerial, satellite and ground observations across forest types and biomes. This includes both improved positioning technologies and standardized protocols that explicitly address the mismatch between point- and plot-based field data and crown- or area-based aerial observations (Leitão et al., 2018). Several authors have emphasized the lack of suitable reference data and stressed the need for harmonized global mortality datasets (Allen et al., 2010; McDowell et al., 2016; Buras et al., 2020; Schuldt et al., 2020). Initiatives such as the International Tree Mortality Network are moving towards such harmonization (Hammond et al., 2022), but large-scale, spatially explicit integration of aerial and ground data remains a long-term goal (International Tree Mortality Network et al., 2025). Progress in this direction would substantially enhance both the validation of remote sensing products and the ability to link mortality to carbon fluxes, thereby advancing our understanding of forest mortality dynamics and their role in the Earth system. In the future, platforms such as deadtrees.earth could contribute to this goal by not only hosting remote sensing products but also accommodating ground-based mortality observations, thereby providing the technological interface needed to connect field data with remote sensing products.

3.4. Applications of global tree mortality products

Global, high-quality tree mortality products derived from aerial and satellite imagery can be used with environmental layers to attribute mortality dynamics to respective drivers and understand the variation in tree mortality dynamics (Schiefer et al., 2024). The variety of global tree mortality products that can be derived from the database will be a key component in enabling researchers to answer pressing questions: *Why are trees dying in the first place and how do the drivers (co)vary across tree species, ecosystems, or biomes? Why do some areas experience excess tree mortality while similar areas experience greening? Is tree mortality dependent upon the species or diversity of neighboring trees? What is the anthropogenic contribution to excess tree mortality? How long does standing deadwood remain in different ecosystems and does this relate to large-scale carbon balances? Where can tree mortality be attributed to global warming and climate extremes? Do the latter factors facilitate (invasive) pests and pathogens?* Given high product quality and increasing global coverage, we hope to support research on tree mortality from a local to a global scale and across biomes.

For example, one can combine standing deadwood maps with large-scale biomass maps (Santoro et al., 2020; Shendryk, 2022) to facilitate our understanding of carbon fluxes. Given the temporal dynamics of standing deadwood, we can compare results to the outputs of vegetation models (*e.g.,* Köhler and Huth, 1998). Thereby, using remote sensing derived products to evaluate and also fine-tune or initialize

parameterizations of vegetation models. Beyond Now- and Hindcasting, Forecasting of tree mortality should be possible if the community finds effective environmental predictors such that tree mortality dynamics for the subsequent year can be modeled.

Beyond tree mortality applications, we envision the orthophoto database to be used in a variety of other use cases. Since in general, this is a centimeter-scale orthophoto database of forests, one can also attempt to detect tree species, analyze tree line patterns, derive tree/non-tree products, pioneer studies on tree health, tree phenology, or attempt to track forest cover dynamics. Broadly speaking the general workflow (see Fig. 7) of upscaling to global products can also be attempted for the same use cases. Especially suited may be forest cover products, tree species distribution maps, or revealing tree loss by forest management or disturbances.

4. Conclusions

The deadtrees.earth database is a centimeter-scale orthophoto collection with standing deadwood delineations. Already, it comprises 2694 centimeter-scale orthophotos with more than 55,000 manually obtained deadwood labels from the last decade distributed across the entire globe. The dataset has unprecedented coverage, and through machine learning methods and global remote sensing satellite missions, the scientific community can leverage this dataset to create models and global datasets, unlocking the potential to effectively track overstory tree mortality dynamics. Ultimately, these data in concert with environmental layers will enable the scientific community to answer pressing questions on tree mortality. To reach this goal, the platform www.deadtrees.earth encompasses an interactive online system that aims to exploit aerial and satellite imagery for uncovering spatial and temporal patterns of tree mortality at a global scale. The web platform supports and encourages uploading and downloading user-generated orthophotos optionally together with labeled standing deadwood. The vision of this platform is an improved understanding of tree mortality patterns and processes from local to global scales. And this vision can only be accomplished through the collective effort of citizens and researchers. The dynamic nature of this database is meant to continuously increase our capacity to detect and understand tree mortality patterns. We hope that through the services of deadtrees.earth, we can attract ample data input from geographic regions that are currently still underrepresented, *e.g.,* Africa and Asia. Finally, with this initiative, we support the paradigm shift in (FAIR) data-sharing practices in the scientific community.

CRediT authorship contribution statement

Clemens Mosig: Writing – review & editing, Writing – original draft, Visualization, Validation, Software, Resources, Project administration, Methodology, Investigation, Formal analysis, Data curation, Conceptualization. **Janusch Vajna-Jehle:** Writing – review & editing, Visualization, Validation, Software, Resources, Methodology, Investigation, Conceptualization. **Miguel D. Mahecha:** Writing – review & editing, Supervision, Project administration, Methodology, Funding acquisition, Conceptualization. **Yan Cheng:** Writing – review & editing, Data curation, Conceptualization. **Henrik Hartmann:** Writing – review & editing, Conceptualization. **David Montero:** Writing – review & editing, Conceptualization. **Samuli Junttila:** Writing – review & editing, Data curation, Conceptualization. **Stéphanie Horion:** Writing – review & editing, Conceptualization. **Mirela Beloiu Schwenke:** Writing – review & editing, Data curation, Conceptualization. **Michael J. Koontz:** Writing – review & editing. **Teja Kattenborn:** Writing – review & editing, Writing – original draft, Visualization, Validation, Supervision, Resources, Project administration, Methodology, Investigation, Funding acquisition, Formal analysis, Conceptualization. All other authors have curated and contributed data, and revised the manuscript.

Declaration of competing interest

The authors declare that they have no known competing financial interests or personal relationships that could have appeared to influence the work reported in this paper.

Acknowledgments

The study is supported by the deadtrees initiative (https://www.deadtrees.earth). The deadtrees.earth initiative is supported by the Ministry for Food, Rural Areas, and Consumer Protection, Baden-Württemberg, Germany (grant 52-8670.00) and the German Research Foundation via the NFDI4Earth pilot project GeoLabel (DFG project no. 460036893, https://www.nfdi4earth.de/). Moreover, the study has been funded by the German Aerospace Centre (DLR) on behalf of the Federal Ministry for Economic Affairs and Climate Action (BMWK) under the projects *UAVforSAT* (project no. 50EE1909A) and *ML4Earth* (FKZ 50EE2201B). Further funding was received from the German Research Foundation (DFG) under the project *BigPlantSens* (project no. 444524904) and PANOPS (project no. 504978936). Some of the icons were provided by Flaticon. JF acknowledges funding by the German Research Foundation (DFG Project ConFobi, GRK 2123). CM, MDM, CB, and JU acknowledge the financial support by the Federal Ministry of Education and Research of Germany and by Sächsische Staatsministerium für Wissenschaft, Kultur und Tourismus in the programme Center of Excellence for AI-research, Center for Scalable Data Analytics and Artificial Intelligence Dresden/Leipzig, project identification number: ScaDS.AI. CM and MDM thank the European Space Agency for funding the "DeepFeatures" project via the AI4SCIENCE activity. SH and YC are funded by Villum Fonden (DRYTIP project, grant agreement no. 37465) and the University of Copenhagen (PerformLCA project, UCPH Strategic plan 2023 Data+ Pool). We acknowledge the Black Forest National Park Administration as on of the data providers. The research of KCC was carried out at Oak Ridge National Laboratory, which is managed by the University of Tennessee-Battelle, LLC, under contract DE-AC05-00OR22725 with the U.S. Department of Energy. The F.F., H.K., and A.S. acknowledge that the Carbon Map and Model project is made possible through the support of the International Climate Initiative (IKI) by the German Federal Ministry for the Environment, Nature Conservation, Building and Nuclear Safety (BMUB) and the German Development Bank (KfW). The project was developed in collaboration with the following agencies in DRC: The Ministry of Environment and Sustainable Development, Direction des Inventaires et Aménagement Forestiers (DIAF), Direction du Développement Durable (DDD), and Observatoire Satellital des Forets d'Afrique Central (OSFAC). This study was supported by the International Tree Mortality Network (https://tree-mortality.net/). A.G., M.G. and T.K. would like to acknowledge funding by the German Research Foundation (DFG, CRC 1537 ECOSENSE, project number: 459819582) and the assistance of A. Enriquez in data processing. Any use of trade, product, or firm names is for descriptive purposes only and does not imply endorsement by the U.S. Government.

Appendix A. Supplementary data

Supplementary material related to this article can be found online at https://doi.org/10.1016/j.rse.2025.115027.

Data availability

All public data is available on the described platform.

References

Allen, C.D., Breshears, D.D., McDowell, N.G., 2015. On underestimation of global vulnerability to tree mortality and forest die-off from hotter drought in the anthropocene. Ecosphere 6 (8), 1–55.

Allen, C.D., Macalady, A.K., Chenchouni, H., Bachelet, D., McDowell, N., Vennetier, M., Kitzberger, T., Rigling, A., Breshears, D.D., Hogg, E.T., et al., 2010. A global overview of drought and heat-induced tree mortality reveals emerging climate change risks for forests. Forest Ecol. Manag. 259 (4), 660–684.

Anderegg, W.R., Kane, J.M., Anderegg, L.D., 2013. Consequences of widespread tree mortality triggered by drought and temperature stress. Nat. Clim. Chang. 3 (1), 30–36.

Bastos, A., Sippel, S., Frank, D., Mahecha, M.D., Zaehle, S., Zscheischler, J., Reichstein, M., 2023. A joint framework for studying compound ecoclimatic events. Nat. Rev. Earth Environ. 4 (5), 333–350.

Bauman, D., Fortunel, C., Delhaye, G., Malhi, Y., Cernusak, L.A., Bentley, L.P., Rifai, S.W., Aguirre-Gutiérrez, J., Menor, I.O., Phillips, O.L., et al., 2022. Tropical tree mortality has increased with rising atmospheric water stress. Nature 608 (7923), 528–533.

Bhatnagar, S., Puliti, S., Talbot, B., Heppelmann, J.B., Breidenbach, J., Astrup, R., 2022. Mapping wheel-ruts from timber harvesting operations using deep learning techniques in drone imagery. Forestry 95 (5), 698–710.

Buras, A., et al., 2020. Climate change-driven tree mortality: the role of forest management and legacy effects. Global Change Biol. 26, 3060–3075. http://dx.doi.org/10.1111/gcb.15051.

Cheng, Y., Oehmcke, S., Brandt, M., Rosenthal, L., Das, A., Vrieling, A., Saatchi, S., Wagner, F., Mugabowindekwe, M., Verbruggen, W., et al., 2024. Scattered tree death contributes to substantial forest loss in california. Nat. Commun. 15 (1), 641.

Cloutier, M., Germain, M., Laliberté, E., 2023. Quebec Trees Dataset. Zenodo, http://dx.doi.org/10.5281/zenodo.8148479.

Coleman, T.W., Graves, A.D., Heath, Z., Flowers, R.W., Hanavan, R.P., Cluck, D.R., Ryerson, D., 2018. Accuracy of aerial detection surveys for mapping insect and disease disturbances in the United States. Forest Ecol. Manag. 430, 321–336.

Dandois, J.P., Olano, M., Ellis, E.C., 2015. Optimal altitude, overlap, and weather conditions for computer vision UAV estimates of forest structure. Remote. Sens. 7 (10), 13895–13920.

Espírito-Santo, F.D., Gloor, M., Keller, M., Malhi, Y., Saatchi, S., Nelson, B., Junior, R.C.O., Pereira, C., Lloyd, J., Frolking, S., et al., 2014. Size and frequency of natural forest disturbances and the Amazon forest carbon balance. Nat. Commun. 5 (1), 1–6.

Fettig, C., Mortenson, L., Bulaon, B., Foulk, P., 2019. Tree mortality following drought in the central and southern Sierra Nevada, California. US For. Ecol. Manage 432, 164–178.

Frey, J., Kovach, K., Stemmler, S., Koch, B., 2018. UAV photogrammetry of forests as a vulnerable process. A sensitivity analysis for a structure from motion RGB-image pipeline. Remote. Sens. 10 (6), 912.

Garrity, S.R., Allen, C.D., Brumby, S.P., Gangodagamage, C., McDowell, N.G., Cai, D.M., 2013. Quantifying tree mortality in a mixed species woodland using multitemporal high spatial resolution satellite imagery. Remote Sens. Environ. 129, 54–65.

Gentilesca, T., Camarero, J.J., Colangelo, M., Ripullone, F., Nole, A., Nolã, A., et al., 2017. Drought-induced oak decline in the western mediterranean region: an overview on current evidences, mechanisms and management options to improve forest resilience. IForest 10 (5), 796–806.

Ghasemi, M., Latifi, H., Pourhashemi, M., 2022. A novel method for detecting and delineating coppice trees in UAV images to monitor tree decline. Remote. Sens. 14 (23), 5910.

Ghasemi, M., Latifi, H., Pourhashemi, M., 2024a. Integrating UAV and freely available space-borne data to describe tree decline across semi-arid mountainous forests. Environ. Model. Assess. 29 (3), 549–568.

Ghasemi, M., Latifi, H., Shafeian, E., Naghavi, H., Pourhashemi, M., 2024b. A novel linear spectral unmixing-based method for tree decline monitoring by fusing UAV-RGB and optical space-borne data. Int. J. Remote Sens. 45 (4), 1079–1109.

Gora, E.M., Esquivel-Muelbert, A., 2021. Implications of size-dependent tree mortality for tropical forest carbon dynamics. Nat. Plants 7 (4), 384–391.

Hammond, W.M., Williams, A.P., Abatzoglou, J.T., Adams, H.D., Klein, T., López, R., Sáenz-Romero, C., Hartmann, H., Breshears, D.D., Allen, C.D., 2022. Global field observations of tree die-off reveal hotter-drought fingerprint for earth's forests. Nat. Commun. 13 (1), 1761.

Hansen, M.C., Potapov, P.V., Moore, R., Hancher, M., Turubanova, S.A., Tyukavina, A., Thau, D., Stehman, S.V., Goetz, S.J., Loveland, T.R., Kommareddy, A., Egorov, A., Chini, L., Justice, C.O., Townshend, J.R.G., 2013. High-resolution global maps of 21st-century forest cover change. Science 342 (6160), 850–853. http://dx.doi.org/10.1126/science.1244693.

Hartmann, H., Bastos, A., Das, A.J., Esquivel-Muelbert, A., Hammond, W.M., Martínez-Vilalta, J., McDowell, N.G., Powers, J.S., Pugh, T.A., Ruthrof, K.X., et al., 2022. Climate change risks to global forest health: emergence of unexpected events of elevated tree mortality worldwide. Annu. Rev. Plant Biol. 73, 673–702.

Hartmann, H., Battisti, A., Brockerhoff, E.G., Bełka, M., Hurling, R., Jactel, H., Oliva, J., Rousselet, J., Terhonen, E., Ylioja, T., et al., 2025. European forests are under increasing pressure from global change-driven invasions and accelerating epidemics by insects and diseases. J. Kult. 77 (02), 6–24.

Hill, A.P., Nolan, C.J., Hemes, K.S., Cambron, T.W., Field, C.B., 2023. Low-elevation conifers in California's Sierra Nevada are out of equilibrium with climate. PNAS Nexus 2 (2), pgad004.

Hugenholtz, C., Brown, O., Walker, J., Barchyn, T., Nesbit, P., Kucharczyk, M., Myshak, S., 2016. Spatial accuracy of UAV-derived orthoimagery and topography: Comparing photogrammetric models processed with direct geo-referencing and ground control points. Geomatica 70 (1), 21–30.

Hülsmann, L., Bugmann, H., Brang, P., 2017. How to predict tree death from inventory data—lessons from a systematic assessment of European tree mortality models. Can. J. Forest Res. 47 (7), 890–900.

International Tree Mortality Network, Senf, C., Esquivel-Muelbert, A., Pugh, T.A., Anderegg, W.R., Anderson-Teixeira, K.J., Arellano, G., Beloiu Schwenke, M., Bentz, B.J., Boehmer, H.J., et al., 2025. Towards a global understanding of tree mortality. New Phytol..

Johnson, P., Ricker, B., Harrison, S., 2017. Volunteered drone imagery: Challenges and constraints to the development of an open shared image repository.

Junttila, S., Blomqvist, M., Laukkanen, V., Heinaro, E., Polvivaara, A., O'Sullivan, H., Yrttimaa, T., Vastaranta, M., Peltola, H., 2024. Significant increase in forest canopy mortality in boreal forests in southeast Finland. Forest Ecol. Manag. 565, 122020. http://dx.doi.org/10.1016/j.foreco.2024.122020.

Kaartinen, H., Hyyppä, J., Vastaranta, M., Kukko, A., Jaakkola, A., Yu, X., Pyöniemi, V., Liang, X., Holopainen, M., Rönkö, P., et al., 2015. An international comparison of individual tree detection and extraction using airborne laser scanning. Remote. Sens. 7 (1), 159–182. http://dx.doi.org/10.3390/rs70100159.

Kattenborn, T., Leitloff, J., Schiefer, F., Hinz, S., 2021. Review on convolutional neural networks (CNN) in vegetation remote sensing. ISPRS J. Photogramm. Remote Sens. 173, 24–49.

Kattenborn, T., Lopatin, J., Förster, M., Braun, A.C., Fassnacht, F.E., 2019. UAV data as alternative to field sampling to map woody invasive species based on combined Sentinel-1 and Sentinel-2 data. Remote Sens. Environ. 227, 61–73.

Kattenborn, T., Schiefer, F., Frey, J., Feilhauer, H., Mahecha, M.D., Dormann, C.F., 2022. Spatially autocorrelated training and validation samples inflate performance assessment of convolutional neural networks. ISPRS Open J. Photogramm. Remote. Sens. 5, 100018.

Khatri-Chhetri, P., van Wagtendonk, L., Hendryx, S.M., Kane, V.R., 2024. Enhancing individual tree mortality mapping: The impact of models, data modalities, and classification taxonomy. Remote Sens. Environ. 300, 113914.

Köhler, P., Huth, A., 1998. The effects of tree species grouping in tropical rainforest modelling: simulations with the individual-based model FORMIND. Ecol. Model. 109 (3), 301–321.

Koontz, M.J., Latimer, A.M., Mortenson, L.A., Fettig, C.J., North, M.P., 2021. Cross-scale interaction of host tree size and climatic water deficit governs bark beetle-induced tree mortality. Nat. Commun. 12 (1), 129.

Lange, M., Preidl, S., Reichmuth, A., Heurich, M., Doktor, D., 2024. A continuous tree species-specific reflectance anomaly index reveals declining forest condition between 2016 and 2022 in Germany. Remote Sens. Environ. 312, 114323.

Leitão, P.J., Schwieder, M., Pötzschner, F., Pinto, J.R., Teixeira, A.M., Pedroni, F., Sanchez, M., Rogass, C., van der Linden, S., Bustamante, M.M., et al., 2018. From sample to pixel: multi-scale remote sensing data for upscaling aboveground carbon data in heterogeneous landscapes. Ecosphere 9 (8), e02298.

Mahecha, M.D., Bastos, A., Bohn, F., Eisenhauer, N., Feilhauer, H., Hickler, T., Kalesse-Los, H., Migliavacca, M., Otto, F.E.L., Peng, J., et al., 2024. Biodiversity and climate extremes: known interactions and research gaps. Earth's Futur. 12 (6), e2023EF003963.

Mansuy, N., Barredo, J.I., Migliavacca, M., Pilli, R., Leverkus, A.B., Janouskova, K., Mubareka, S., 2024. Reconciling the different uses and values of deadwood in the European green deal. One Earth 7 (9), 1542–1558.

McDowell, N.G., et al., 2016. Multi-scale predictions of massive conifer mortality due to chronic temperature rise. Nat. Clim. Chang. 6, 295–300. http://dx.doi.org/10.1038/nclimate2873.

McRoberts, R.E., Tomppo, E.O., Næsset, E., 2010. Advances and emerging issues in national forest inventories. Scand. J. For. Res. 25 (4), 368–381.

Meyer, H., Pebesma, E., 2022. Machine learning-based global maps of ecological variables and the challenge of assessing them. Nat. Commun. 13 (1), 2208.

Migliavacca, M., Grassi, G., Bastos, A., Cecchirini, G., Ciais, P., Janssens-Maenhout, G., Lugato, E., Mahecha, M.D., Novick, K.A., Peñuelas, J., Pilli, R., Reichstein, M., Avitabile, V., Beck, P.S.A., Barredo, J.L., Forzieri, G., Herold, M., Korosuo, A., Mansuy, N., Mubareka, S., Orth, R., Rougieux, P., Cescatti, A., 2025. Securing the forest carbon sink for the European Union's climate ambition. Nature http://dx.doi.org/10.1038/s41586-025-08967-3, [Accepted 28 March 2025; Received 4 September 2024].

Moghaddas, J., Roller, G., Long, J., Saah, D., Moritz, M., Star, D., Schmidt, D., Buchholz, T., Freed, T., Alvey, E., et al., 2018. Fuel Treatment for Forest Resilience and Climate Mitigation: a Critical Review for Coniferous Forests of California. California Natural Resources Agency, Publication number: CCCA4-CNRA-2018–017.

Möhring, J., Kattenborn, T., Mahecha, M.D., Cheng, Y., Schwenke, M.B., Cloutier, M., Denter, M., Frey, J., Gassilloud, M., Göritz, A., et al., 2025. Global, multi-scale standing deadwood segmentation in centimeter-scale aerial images. Authorea Prepr..

Olson, D.M., Dinerstein, E., Wikramanayake, E.D., Burgess, N.D., Powell, G.V.N., Underwood, E.C., D'amico, J.A., Itoua, I., Strand, H.E., Morrison, J.C., Loucks, C.J., Allnutt, T.F., Ricketts, T.H., Kura, Y., Lamoreux, J.F., Wettengel, W.W., Hedao, P., Kassem, K.R., 2001. Terrestrial Ecoregions of the World: A New Map of Life on Earth: A new global map of terrestrial ecoregions provides an innovative tool for conserving biodiversity. BioScience 51 (11), 933–938. http://dx.doi.org/10.1641/0006-3568(2001)051[0933:TEOTWA]2.0.CO;2.

Pan, Y., Birdsey, R.A., Fang, J., Houghton, R., Kauppi, P.E., Kurz, W.A., Phillips, O.L., Shvidenko, A., Lewis, S.L., Canadell, J.G., et al., 2011. A large and persistent carbon sink in the world's forests. Science 333 (6045), 988–993.

Puletti, N., Canullo, R., Mattioli, W., Gawryś, R., Corona, P., Czerepko, J., 2019. A dataset of forest volume deadwood estimates for Europe. Ann. For. Sci. 76, 1–8.

Puliti, S., Breidenbach, J., Astrup, R., 2020. Estimation of forest growing stock volume with UAV laser scanning data: can it be done without field data? Remote. Sens. 12 (8), 1245.

Puliti, S., Solberg, S., Granhus, A., 2019. Use of UAV photogrammetric data for estimation of biophysical properties in forest stands under regeneration. Remote. Sens. 11 (3), 233.

Purfürst, T., 2022a. Evaluation of static autonomous GNSS positioning accuracy using Single-, Dual-, and Tri-frequency smartphones in forest canopy environments. Sensors 22 (3), 1289.

Purfürst, F.T., 2022b. Waldmesslehre: Grundlagen Und Anwendungen Forstlicher Messtechnik. Springer Spektrum, Berlin, Heidelberg, http://dx.doi.org/10.1007/978-3-662-63984-4.

Rossi, C., Wiesmann, S., 2024. Flying high for conservation: Opportunities and challenges of operating drones within the oldest national park in the alps. Ecol. Solut. Evid. 5 (2), e12354.

Santoro, M., Cartus, O., Carvalhais, N., Rozendaal, D., Avitabilie, V., Araza, A., De Bruin, S., Herold, M., Quegan, S., Rodríguez Veiga, P., et al., 2020. The global forest above-ground biomass pool for 2010 estimated from high-resolution satellite observations. Earth Syst. Sci. Data Discuss. 2020, 1–38.

Scheffer, M., Carpenter, S., Foley, J.A., Folke, C., Walker, B., 2001. Catastrophic shifts in ecosystems. Nature 413 (6856), 591–596.

Schiefer, F., Schmidtlein, S., Frick, A., Frey, J., Klinke, R., Zielewska-Büttner, K., Junttila, S., Uhl, A., Kattenborn, T., 2023. UAV-based reference data for the prediction of fractional cover of standing deadwood from sentinel time series. ISPRS Open J. Photogramm. Remote. Sens. 8, 100034.

Schiefer, F., Schmidtlein, S., Hartmann, H., Schnabel, F., Kattenborn, T., 2024. Large-scale remote sensing reveals that tree mortality in Germany appears to be greater than previously expected. For. Int. J. For. Res. cpae062. http://dx.doi.org/10.1093/forestry/cpae062.

Schuldt, B., et al., 2020. Tree mortality: A key driver of terrestrial carbon cycling. Nat. Plants 6, 10–12. http://dx.doi.org/10.1038/s41477-019-0627-6.

Schwarz, S., Werner, C., Fassnacht, F.E., Ruehr, N.K., 2024. Forest canopy mortality during the 2018–2020 summer drought years in central Europe: The application of a deep learning approach on aerial images across Luxembourg. For. Int. J. For. Res. 97 (3), 376–387.

Senf, C., Buras, A., Zang, C.S., Rammig, A., Seidl, R., 2020. Excess forest mortality is consistently linked to drought across Europe. Nat. Commun. 11 (1), 6200.

Senf, C., Pflugmacher, D., Zhiqiang, Y., Sebald, J., Knorn, J., Neumann, M., Hostert, P., Seidl, R., 2018. Canopy mortality has doubled in Europe's temperate forests over the last three decades. Nat. Commun. 9 (1), 4978.

Senf, C., Seidl, R., 2021. Mapping the forest disturbance regimes of Europe. Nat. Sustain. 4 (1), 63–70.

Shendryk, Y., 2022. Fusing GEDI with earth observation data for large area aboveground biomass mapping. Int. J. Appl. Earth Obs. Geoinf. 115, 103108.

Stephens, S.L., Bernal, A.A., Collins, B.M., Finney, M.A., Lautenberger, C., Saah, D., 2022. Mass fire behavior created by extensive tree mortality and high tree density not predicted by operational fire behavior models in the southern Sierra Nevada. Forest Ecol. Manag. 518, 120258.

Stephens, S.L., Collins, B.M., Fettig, C.J., Finney, M.A., Hoffman, C.M., Knapp, E.E., North, M.P., Safford, H., Wayman, R.B., 2018. Drought, tree mortality, and wildfire in forests adapted to frequent fire. BioScience 68 (2), 77–88.

Stephenson, N.L., Das, A.J., Ampersee, N.J., Bulaon, B.M., Yee, J.L., 2019. Which trees die during drought? The key role of insect host-tree selection. J. Ecol. 107 (5), 2383–2401.

Stewart, A.J., Robinson, C., Corley, I.A., Ortiz, A., Ferres, J.M.L., Banerjee, A., 2022. Torchgeo: deep learning with geospatial data. In: Proceedings of the 30th International Conference on Advances in Geographic Information Systems. pp. 1–12.

Tang, L., Shao, G., 2015. Drone remote sensing for forestry research and practices. J. For. Res. 26, 791–797.

Thonfeld, F., Gessner, U., Holzwarth, S., Kriese, J., da Ponte, E., Huth, J., Kuenzer, C., 2022. A first assessment of canopy cover loss in Germany's forests after the 2018–2020 drought years. Remote. Sens. 14 (3), http://dx.doi.org/10.3390/rs14030562.

Trugman, A.T., Anderegg, L.D., Anderegg, W.R., Das, A.J., Stephenson, N.L., 2021. Why is tree drought mortality so hard to predict? Trends Ecol. Evolut. 36 (6), 520–532.

Trumbore, S., Brando, P., Hartmann, H., 2015. Forest health and global change. Science 349 (6250), 814–818.

Valbuena, R., Mauro, F., Rodriguez-Solano, R., Manzanera, J.A., 2010. Practical accuracy assessment of GNSS receivers and laser rangefinders for forestry applications. Comput. Electron. Agric. 73 (3), 244–253. http://dx.doi.org/10.1016/j.compag.2010.06.006.

Vasquez, V., Garcia, M., Hernandez, M., Muller-Landau, H.C., 2023. Barro Colorado Island 50-ha plot aerial photogrammetry orthomosaics and digital surface models for 2018–2023: Globally and locally aligned time series.. http://dx.doi.org/10.25573/data.24782016.v1, https://smithsonian.figshare.com/articles/dataset/Barro_Colorado_Island_50-ha_plot_aerial_photogrammetry_orthomosaics_and_digital_surface_models_for_2018-2023_Globally_and_locally_aligned_time_series_/24782016.

Vilanova, E., Mortenson, L.A., Cox, L.E., Bulaon, B.M., Lydersen, J.M., Fettig, C.J., Battles, J.J., Axelson, J.N., 2023. Characterizing ground and surface fuels across Sierra Nevada forests shortly after the 2012–2016 drought. Forest Ecol. Manag. 537, 120945.

Watt, M.S., Holdaway, A., Watt, P., Pearse, G.D., Palmer, M.E., Steer, B.S.C., Camarretta, N., McLay, E., Fraser, S., 2024. Early prediction of regional red needle cast outbreaks using climatic data trends and satellite-derived observations. Remote. Sens. 16 (8), http://dx.doi.org/10.3390/rs16081401.

Werner, C., Wallrabe, U., Christen, A., Comella, L., Dormann, C., Göritz, A., Grote, R., Haberstroh, S., Jouda, M., Kiese, R., et al., 2024. ECOSENSE-Multi-scale quantification and modelling of spatio-temporal dynamics of ecosystem processes by smart autonomous sensor networks. Res. Ideas Outcomes 10, e129357.

Wilkinson, M.D., Dumontier, M., Aalbersberg, I.J., Appleton, G., Axton, M., Baak, A., Blomberg, N., Boiten, J.-W., da Silva Santos, L.B., Bourne, P.E., et al., 2016. The FAIR guiding principles for scientific data management and stewardship. Sci. Data 3 (1), 1–9.

Winter, C., Mueller, S., Kattenborn, T., Stahl, K., Szillat, K., Weiler, M., Schnabel, F., 2024. Forest dieback in drinking water protection areas–a hidden threat to water quality. BioRxiv, 2024-2008.

Woodall, C., Grambsch, P., Thomas, W., 2005. Applying survival analysis to a large-scale forest inventory for assessment of tree mortality in Minnesota. Ecol. Model. 189 (1–2), 199–208.

Xu, L., Saatchi, S.S., Shapiro, A., Meyer, V., Ferraz, A., Yang, Y., Bastin, J.-F., Banks, N., Boeckx, P., Verbeeck, H., et al., 2017. Spatial distribution of carbon stored in forests of the democratic Republic of Congo. Sci. Rep. 7 (1), 15030.

Yan, Y., Piao, S., Hammond, W.M., Chen, A., Hong, S., Xu, H., Munson, S.M., Myneni, R.B., Allen, C.D., 2024. Climate-induced tree-mortality pulses are obscured by broad-scale and long-term greening. Nat. Ecol. Evol. 8 (5), 912–923.

Zanaga, D., Van De Kerchove, R., Daems, D., De Keersmaecker, W., Brockmann, C., Kirches, G., Wevers, J., Cartus, O., Santoro, M., Fritz, S., et al., 2022. ESA WorldCover 10 m 2021 v200.

Zeng, Y., Hao, D., Huete, A., Dechant, B., Berry, J., Chen, J.M., Joiner, J., Frankenberg, C., Bond-Lamberty, B., Ryu, Y., et al., 2022. Optical vegetation indices for monitoring terrestrial ecosystems globally. Nat. Rev. Earth Environ. 3 (7), 477–493.

Zhang, H.K., Camps-Valls, G., Liang, S., Tuia, D., Pelletier, C., Zhu, Z., 2025. Preface: Advancing deep learning for remote sensing time series data analysis.

Zhang, X., Friedl, M., Henebry, G., 2020. VIIRS/NPP Land Cover Dynamics Yearly L3 Global 500 m SIN Grid V001 [Data set]. http://dx.doi.org/10.5067/VIIRS/VNP22Q2.001.

Zhang, X., Jayavelu, S., Liu, L., Friedl, M.A., Henebry, G.M., Liu, Y., Schaaf, C.B., Richardson, A.D., Gray, J., 2018. Evaluation of land surface phenology from VIIRS data using time series of PhenoCam imagery. Agricult. Forest. Meterol. 256, 137–149.